



## Revolutionizing heat recovery in shell-and-tube latent heat storage systems: an arc-shaped fin approach

Mohamed Boujelbene, Jasim M. Mahdi, Anmar Dulaimi, Hosseinali Ramezanimouziraji, Raed Khalid Ibrahim, Raad Z. Homod, Wahiba Yaïci, Pouyan Talebizadehsardari & Amir Keshmiri

**To cite this article:** Mohamed Boujelbene, Jasim M. Mahdi, Anmar Dulaimi, Hosseinali Ramezanimouziraji, Raed Khalid Ibrahim, Raad Z. Homod, Wahiba Yaïci, Pouyan Talebizadehsardari & Amir Keshmiri (2023) Revolutionizing heat recovery in shell-and-tube latent heat storage systems: an arc-shaped fin approach, Engineering Applications of Computational Fluid Mechanics, 17:1, 2255036, DOI: [10.1080/19942060.2023.2255036](https://doi.org/10.1080/19942060.2023.2255036)

**To link to this article:** <https://doi.org/10.1080/19942060.2023.2255036>



© 2023 The Author(s). Published by Informa UK Limited, trading as Taylor & Francis Group.



Published online: 12 Sep 2023.



Submit your article to this journal [↗](#)



Article views: 471



View related articles [↗](#)



View Crossmark data [↗](#)

# Revolutionizing heat recovery in shell-and-tube latent heat storage systems: an arc-shaped fin approach

Mohamed Boujelbene<sup>a</sup>, Jasim M. Mahdi<sup>b</sup>, Anmar Dulaimi<sup>c</sup>, Hosseinali Ramezanimouziraji<sup>d</sup>,  
Raed Khalid Ibrahim<sup>e</sup>, Raad Z. Homod<sup>f</sup>, Wahiba Yaïci<sup>g</sup>, Pouyan Talebizadehsardari<sup>h</sup> and Amir Keshmiri<sup>i</sup>

<sup>a</sup>Industrial Engineering Department, College of Engineering, University of Ha'il, Ha'il, Saudi Arabia; <sup>b</sup>Department of Energy Engineering, University of Baghdad, Baghdad, Iraq; <sup>c</sup>College of Engineering, University of Warith Al-Anbiya, Karbala, Iraq; <sup>d</sup>Department of Mechanical Engineering, Tarbiat Modares University, Tehran, Iran; <sup>e</sup>Department of Medical Instrumentation Engineering, Al-Farahidi University, Baghdad, Iraq; <sup>f</sup>Department of Oil and Gas Engineering, Basrah University for Oil and Gas, Basra, Iraq; <sup>g</sup>CanmetENERGY Research Centre, Natural Resources Canada, Ottawa, Canada; <sup>h</sup>Power Electronics, Machines and Control (PEMC) Research Group, University of Nottingham, Nottingham, UK; <sup>i</sup>ManchesterCFD Team, Department of Fluids & Environment, School of Engineering, University of Manchester, Manchester, UK

## ABSTRACT

Strengthening the thermal response of Phase-Change Materials (PCMs) is an essential and active field of research with promising potential for advanced applications such as solar energy storage, building energy conservation, and thermal management in electronic devices. This article evaluates the efficacy of a new arc-shaped fin array in shell-and-tube heat storage systems to enhance the PCM response during the discharge mode. Different fin geometric parameters including the fin curvature angle, the fin spacing, and the nonuniform angle between fins in the top and bottom sections of the PCM domain were considered to identify the best-performing layout. The analysis shows that increasing the curvature of arc-shaped fins between 60° and 180° and increasing the fin spacing between 5 and 15 mm can significantly reduce solidifying time and improve heat recovery rates. Moreover, the arc-shaped fins are more efficient than conventional longitudinal (+-shaped) fins, which are commonly employed in thermal energy storage applications. Arc-shaped fins can also save discharge time by more than half and improve the rate of heat recovery by almost four times than that of +-shaped fins. The present findings suggest that arc-shaped fins represent a promising design for enhancing the heat-recovery aspects in PCM-based energy storage systems.

## ARTICLE HISTORY

Received 20 June 2023  
Accepted 30 August 2023





## KEYWORDS

Computational fluid dynamics; latent heat storage; solidification; enhancement; phase change materials; fins

## 1. Introduction

As per a recent report by the International Energy Agency (IEA, 2023), global energy-related carbon emissions surged to a new peak of over 36.8 Gt in 2022, indicating a yearly rise of 0.9% or 321 Mt. Around 224 Mt of this rise can be attributed to coal-fired electricity and heat generation (Lu et al., 2018). The most reliable path to limit the resurgence in coal power emissions is through the expansion of renewable energy generation (IRENA, 2020a). However, the adoption of renewable energy is hampered by a significant barrier which is the intermittent energy supply (Huang et al., 2020). This intermittency poses challenges in maintaining a reliable power supply, especially in grid systems designed around constant energy input (Gong et al., 2022; Xu et al., 2022). These challenges can be overcome through improvements in energy storage technologies, such as Thermal

Energy Storage (TES), which can effectively preserve surplus energy generated during periods of high production for use during times of low production (IRENA, 2020b; Wen et al., 2021). This enables a more stable and reliable supply of energy, which is essential for meeting the growing demand for energy from clean and alternative energy resources (Wu, Li, et al., 2021; Wu, Zhao, et al., 2021). By providing a consistent energy output, TES reduces the need for costly fossil fuel imports and mitigates their environmental damaging impact (Rashid et al., 2023; Song et al., 2023). TES systems come in various forms – thermochemical, latent, and sensible – which are characterized based on the type of working material in use (Wang, Fu, et al., 2023). Among these, latent TES stands out due to its use of phase-change materials (PCMs), which offer some significant advantages. For instance, solid-liquid PCMs operate on an

**CONTACT** Pouyan Talebizadehsardari  pouyan.talebizadehsardari2@nottingham.ac.uk  Power Electronics, Machines and Control (PEMC) Research Group, University of Nottingham, Nottingham, UK; Amir Keshmiri  a.keshmiri@manchester.ac.uk  ManchesterCFD Team, Department of Fluids & Environment, School of Engineering, University of Manchester, Manchester, M13 9PL, UK

© 2023 The Author(s). Published by Informa UK Limited, trading as Taylor & Francis Group.  
This is an Open Access article distributed under the terms of the Creative Commons Attribution License (<http://creativecommons.org/licenses/by/4.0/>), which permits unrestricted use, distribution, and reproduction in any medium, provided the original work is properly cited. The terms on which this article has been published allow the posting of the Accepted Manuscript in a repository by the author(s) or with their consent.

energy absorption and dissipation cycle, wherein they absorb energy during the melting phase and dissipate it upon solidification (Rashid et al., 2023). This means that they can store thermal energy in the form of latent heat, which is much more efficient than storing energy in the form of sensible heat. This property renders PCM-based TES systems superior in terms of storage density. Compared to rock-based TES systems, those employing PCMs offer storage densities that are approximately 1–17 times greater, as elucidated by (Lane, 1983). Another advantage, the solid-to-liquid transition in PCMs results in minimal temperature degradation, allowing the storage system to proceed to work with almost no temperature shifts (Zhao et al., 2019).

The primary challenge that most PCMs used in heat storage systems face is their low thermal conductivity. This affects the response rates during energy charge and discharge modes, leading to lower energy performance in practical applications (Wang et al., 2018). To address this issue, several enhancement materials are used to enhance thermal conductivity to form well-performing PCM systems. These materials include nanoparticles (Mahdi & Nsofor, 2018), micro or nano-encapsulation (Ghalambaz et al., 2019), extended fins (Wang, Lei, et al., 2023), and porous foams (Du et al., 2023). Fins are gaining popularity for application in PCM systems to improve their energy storage/recovery responsiveness due to their cost effectiveness, easy installation, and superb performance boost (Agyenim et al., 2009; Hosseinzadeh et al., 2021). Fins are thin metal structures that extend from the thermally active wall into the PCM for increasing the surface area available for heat communication between the PCM and the heat transfer fluid in use. The increased surface area allows for improving the heat exchange rate, boosting the heat diffusion through PCM, and homogenizing the temperature distribution within the PCM zone. Thus, the introduction of fins expedite the phase transition of PCM and enhance the overall effectiveness of the latent TES system (Zhang, Mancin, et al., 2023). There are numerous types and configurations of fins that can be used for PCM-based TES, such as rectangular (Rathod & Banerjee, 2015), annular (Bahlekeh et al., 2022), pin (Rajabifar et al., 2016), twisted (Mashayekhi et al., 2022), tree-shaped (Peng et al., 2022), etc. (Khedher et al., 2023; Khosravi et al., 2023). The design and optimization of fins depend on several factors, such as the geometry, size, number, spacing, orientation, material, and shape of the fins, as well as the properties of the PCM and the heat transfer fluid (HTF) (Wang et al., 2022).

Several studies were conducted earlier by researchers to verify the efficacy of fins in enhancing thermal response and energy storage rate of PCMs. Mahdi and Nsofor (2018) evaluated three techniques to enhance the

solidification of PCMs: nanoparticles alone, fins alone, and a combination of both. To quantify volume reductions on the PCM side, they used specific measures:  $\phi_n$  for nanoparticle volume fraction,  $\phi_f$  for fin volume fraction, and  $\phi_t$  for the volume fraction of the nanoparticle-fin combination. Their findings indicated that nanoparticles, whether used independently or in conjunction with fins, significantly accelerated the solidification process. However, when considering equivalent reductions in the available PCM volume, the use of fins alone was superior in enhancing the solidification rate. Mozafari, Hooman, et al. (2022) demonstrated that a dual-PCM arrangement reduces the total charging–discharging time by approximately 14% in comparison to the conventional single-PCM arrangement. Furthermore, their results indicated that the integration of fins with a low volume concentration (4%) offers superior performance over nanoparticles, assuming the same volume of PCMs in use. Zhang, Cao, et al. (2023) demonstrated that the dispersion of nanoparticles at a volumetric concentration of 5% could enhance discharging performance of paraffin RT-82 by about 9%. However, a more substantial improvement of about 85% was achieved when the nanoparticles combined with an array of branch-structured fins.

Over the past decade, a number of researchers have a wide range of fin arrangements and evaluated their efficacy in detail. One study by Hosseini et al. (2015) assessed the improved efficiency of a PCM system utilizing various rectangular fin patterns. The study revealed that the utilization of rectangular fins can notably enhance the heat diffusion into the PCM, leading to a considerable improvement in the melting rate, particularly when an optimal fin height is employed. Another study by Abdulateef et al. (2018) conducted on the utilization of triangular fins in a triplex-tube storage device. The study indicated a 15% increase in heat charging rate when triangular fins were employed, compared to rectangular fins. Apart from rectangular and triangular fins, various other types of fins have been examined as well. Hassan et al. (2020) tested the efficiency of a latent storage system with rectangular and annular fin configurations. The results showed that the use of annular fins can improve the melting rate by about 70% in the system with annular fins and 55% in the system with rectangular fins, as compared to the system with no fins. The enhancement of melting in a PCM with annular fins was also evaluated in a study conducted by Yang et al. (2017). The research findings indicate that the integration of annular fins with appropriate geometric characteristics can enhance the rate of melting by up to 65% in comparison to the system of no fins. Sciakovelli et al. (2015) proposed the implementation of tree-shaped fins to enhance the low solidification rate of PCMs. The authors found that expanded angles between

the fin branches were more beneficial for short-term operations, whereas reduced angles were more advantageous for long-term operations. Bo et al. (2022) suggested the application of twisted fins as a means of enhancing the low solidification efficiency of PCM systems. The results showed that the use of twisted fins for the same amount of PCM material can increase the heat recovery rate by 55% as compared to the rectangular fins.

Although employing fins in PCM systems is useful, there are several challenges that need addressing. The optimal design, orientation, and arrangement of the fins are among the challenges that must be addressed. The fins must be designed, arranged, and oriented in a manner that optimizes the surface area in contact with PCM while minimizing the impact on the buoyancy-driven flow of the liquid PCM (Mahdi et al., 2019). Due to their rigid structure, fins impose high flow-resistant forces, which alters the positive role of natural convection. This can be a complex process that requires rigorous analysis of trade-offs between system requirements and limitations. One remedy is to use non-uniform fin arrangements to provide more homogeneous heat dispersion across the different PCM zones. A pioneer study by Mahdi et al. (2018) showed that the use of nonuniform lengths and numbers of rectangular fins between the top and bottom sections of the PCM domain can secure a compromise between the suppression of natural convection by the solid fin structure and the augmentation of thermal conduction due to the added heat-transfer area by the fin addition. A study by Wu et al. (2022) confirmed that the use of fins can improve the heat storage rate by about 104% for non-uniform fin length and distribution, and 61% for uniform fin length and distribution as compared to the system of no fins. Tang et al. (2021) showed that the heat storage time of horizontal shell-and-tube TES systems could be greatly improved by employing non-uniform fin layouts, with fin heights a bit less than the radii of outer pipe with more fins localized in the lower region of the PCM domain. Ao et al. (2023) showed that applying non-uniform distribution of annular fins to shell-and-tube storage unit with 70°-inclination improved the heat transfer and the heat storage time by about 53% and 21% compared to the case of uniform fin distribution.

Inspired by the ongoing efforts to develop efficient enhancement additives for overcoming the slow response times and low efficiency of latent TES systems, this study intends to explore the improved discharging rates in the shell-and-tube type of PCM-based storage systems by employing new arc-shaped fins. To determine the most effective fin layout and distribution for different thermofluidic conditions of the PCM in use, several parametric investigations were conducted using the same

volume for the fin sections. The goal was to optimize the dimensions, orientation, and arrangement of the arc-shaped fins to achieve optimal results in heat removal and energy discharging in latent TES systems. From a design perspective, the strategy of augmenting the discharging rate of PCMs by incorporating enhancers, particularly fins, holds critical importance. This importance arises from the observation that heat transfer rate during the solidification of PCM is typically slower than during melting, largely due to the less effective role of natural convection during solidification (Cabeza, 2021; Tao et al., 2017). As such, a computational fluid mechanics (CFD) based simulation model was developed and validated considering the convective flow conditions and the temperature dependent properties of PCM. The study mainly explored the effects of arc-shaped fin geometric parameters including the fin curvature angle, the spacing of fin base, and the nonuniform angle between fins in the top and bottom regions of the PCM domain. The best-performing fin layout was determined by analyzing various performance indicators such as the solidifying time, temperature distribution, and heat recovery rates. The study would provide valuable insights for designing efficient storage systems that can meet the needs of various engineering applications under different operating conditions.

## 2. Physical model and methodology

The primary aim of this work is to optimize the solidification behavior of PCM within a horizontal latent heat shell-and-tube heat exchanger. This has been achieved by introducing a novel design of arc-shaped fins, fabricated from copper, which are attached to the inner tube. The arc-shaped fins are basically sectors of a circle with varying angles. The inner tube is considered to have a radius of 19 mm and a thickness of 1 mm, while the outer shell has a radius of 40 mm. The annular space between the inner tube and outer shell is filled with the PCM, while the working fluid flows through the inner tube. To maintain a nearly constant temperature within the tube, the working fluid is circulated inside the tube with an appropriate flow rate. Due to the symmetry along the vertical direction, the computational domain for numerical simulation is limited to a specific section of the heat exchanger. Figure 1 depicts the geometries of the cases under investigation. The cases are as follows:

- a) Without arc-shaped fins
- b) With a single arc-shaped fin
- c) With three arc-shaped fins
- d) With four arc-shaped fins

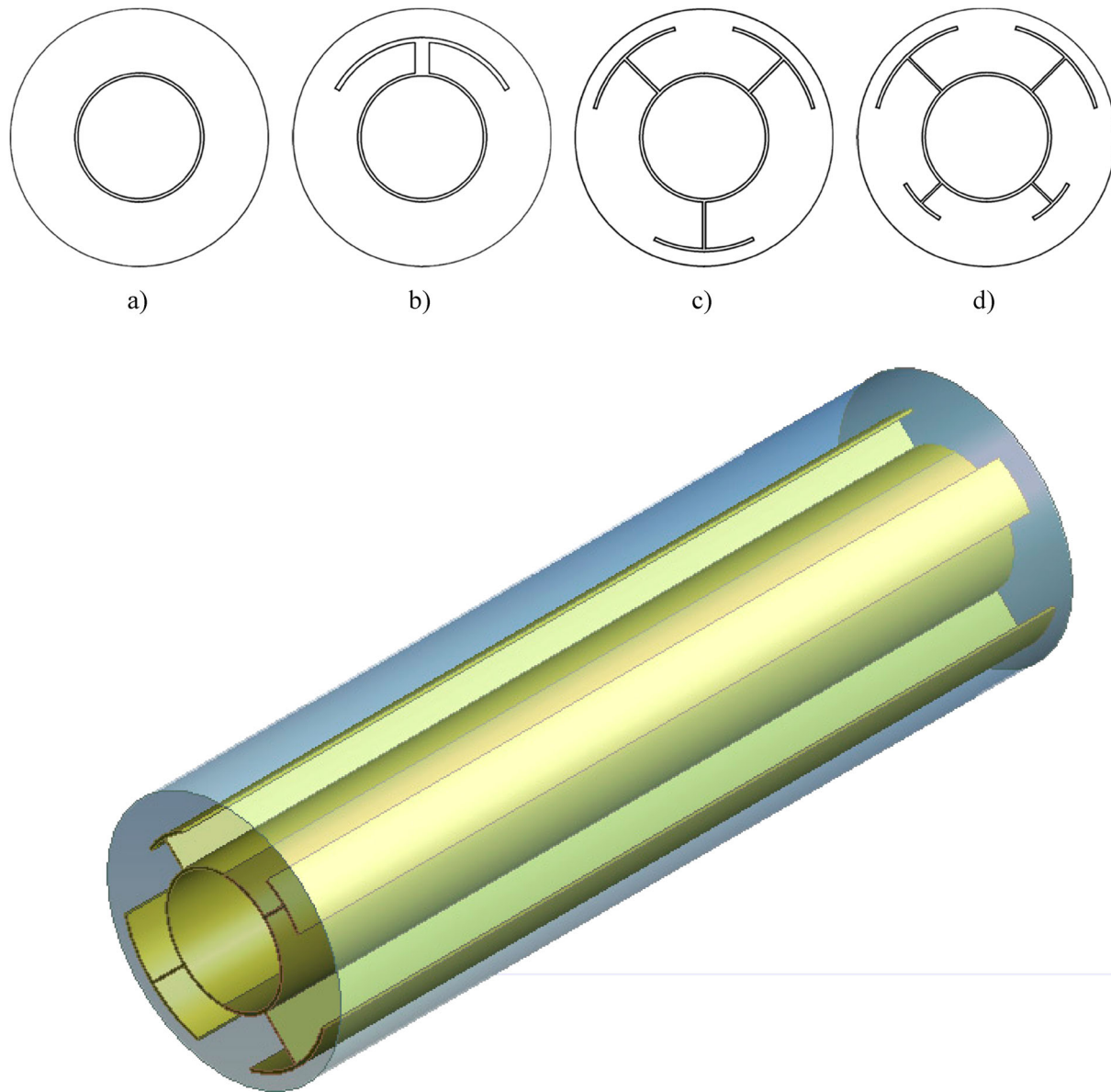


**Figure 1.** The schematic of the studied geometries including the cases with a) no fin, b) one arc-shaped fin, c) three arc-shaped fins and d) four arc-shaped fins.

It is important to note that in Figure 1c, the configuration with two fins is achieved by connecting the fins at the top of the heat exchanger.

As shown in the literature for a shell-and-tube heat exchanger with no-fins, the appropriate distribution of fins within the PCM domain hinges on the predominant mode of heat transfer. For In melting mode, natural convection plays a more prominent role, and melting occurs more swiftly in the upper half due to the significant effect of local natural convection, then an increase in the volume fraction of fins in the lower half is recommended (Mahdi et al., 2018, 2019). This strategy promotes a more uniform propagation of melting across the entire PCM domain. Conversely, in solidification

mode, natural convection is less effective, and solidification proceeds more rapidly in the lower half due to the substantial effect of local conduction, then an increase of the fin volume fraction in the upper half is recommended to facilitate a more uniform propagation of solidification throughout the entire PCM domain. Therefore, the configuration and number of the fins were changed to find the optimum case toward the best solidification performance. A systematic analysis of various parameters related to the optimization of fin design used in the system was performed. The design variables considered are the radial angle of the fins, the number of fins, and the length of the fin's base (the distance from the inner tube to the curved part of the



fins). The following steps were followed to examine these variables:

- Step 1: Radial angles of the fins are studied by considering three angles: 60°, 120°, and 180°.
- Step 2: The length of the fin's base is studied to determine the optimal value based on the best case identified in the previous step.
- Step 3: The radial angle between the fins placed at the bottom of the inner pipe was studied. This analysis considered three fins with equal volume.
- Step 4: Similarly, the radial angle between the fins placed at the top of the inner pipe is studied, this time with four fins having the same volume.

The optimal position and geometry of the fins are obtained by performing the above procedure. For the sake of a meaningful comparison, all the cases studied are designed to maintain a constant volume for the fin sections. Figure 2 illustrates the parameters evaluated during the optimization process, and Table 1 provides the corresponding values for the different cases shown in Figure 2. It is worth mentioning that, in the case where the number of fins is 3 and  $\alpha = 0$ , the fins at the bottom are merged, effectively reducing the number of fins to 2. The selected values highlighted in red represent the best choices for each part of the analysis. A more comprehensive discussion and detailed results can be found in the results and discussion section.

RT35 is used as the PCM inside the heat storage unit to store heat which has a melting point suitable for solar

**Table 1.** The proposed values for different studied parameters in this study.

	Number of fins	$\delta$	$\sum \alpha$	B	$\gamma$
Scenario 1	1	10	60 120 180	0	0
Scenario 2	1	5 10 15	180	0	0
Scenario 3	3	15	180	0 30 60	0
Scenario 4	4	15	180	30	30 60 120

**Table 2.** Thermal characteristics of the PCM, as sourced from the manufacture (GmbH).

Properties	Values
$\rho$ [kg/m <sup>3</sup> ]	770 in solid state / 860 in liquid state
$L_f$ [kJ/kg]	160
$C_p$ [J/kg°C]	2000
$K$ [W/m°C]	0.2
$\mu$ [N.s/m <sup>2</sup> ]	0.023
$T_m$ [°C]	36 (liquidus temperature)/29 (Solidus temperature)
$\beta$ [°C <sup>-1</sup> ]	0.06

energy applications integrated with building. Table 2 is a list of RT35's characteristics, as provided by its manufacturer, Rubitherm (GmbH).

### 3. Numerical model

#### 3.1. Governing equations

For incompressible liquid PCM, the continuity equation can be given as:

$$\nabla \cdot \vec{V} = 0 \quad (1)$$

The Boussinesq simplification that is often used in natural convection problems, where the fluid density is assumed to be constant everywhere, except in the gravity term of the momentum equation, where it is proportional to the temperature difference from a reference value. This way, the fluid can be treated as incompressible, but still accounts for the buoyancy effects that drive the convection. Using this approximation, the momentum equation for fluid flow of PCM is formulated as (Li et al., 2023):

$$\begin{aligned} \rho \frac{\partial \vec{V}}{\partial t} + \rho (\vec{V} \cdot \nabla) \vec{V} \\ = -\nabla P + \mu (\nabla^2 \vec{V}) - \rho \beta (T - T_{ref}) \vec{g} \\ - A_m \frac{(1 - \lambda)^2}{\lambda^3 + 0.001} \vec{V} \end{aligned} \quad (2)$$

The third and fourth terms of Equation 2 are related to the buoyancy effect and phase change process. The buoyancy term accounts for the density difference between the fluid and the solid due to temperature and concentration gradients. The phase change term represents the momentum source or sink caused by the latent heat release at the solid-liquid interface. Based on the enthalpy-porosity method, the phase change term is calculated considering

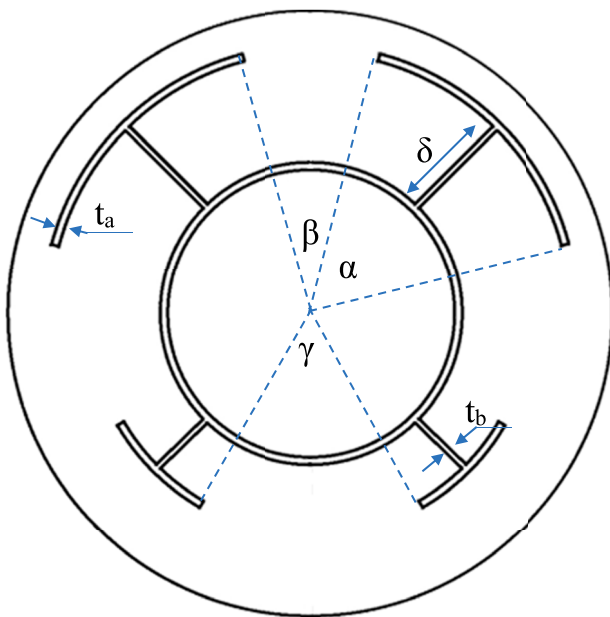


**Figure 2.** The geometrical parameters assessed in this study.

mushy zone factor  $A_m$  of  $10^5$  which is determined based on the validation with literature (Al-Abidi et al., 2014).

In the momentum equation, the melt fraction ( $\lambda$ ) can be calculated based on the temperature of PCM as follows (Brent et al., 1988):

$$\lambda = \frac{\Delta H}{L_f} = \begin{cases} 0 & \text{if } T < T_s \\ \frac{T - T_s}{T_L - T_s} & \text{if } T_s \leq T \leq T_L \\ 1 & \text{if } T > T_L \end{cases} \quad (3)$$

To determine the temperature of the PCM, the energy balance equations is given as (Mozafari, Lee, et al., 2022):

$$\begin{aligned} \frac{\rho C_p \partial T}{\partial t} + \rho C_p \nabla(\vec{V}T) \\ = k \nabla(\nabla T) - \frac{\rho L_f \partial \lambda}{\partial t} + \rho L_f \nabla(\vec{V}\lambda) \end{aligned} \quad (4)$$

The storage level of PCM is the sum of its sensible heat storage (MC<sub>p</sub>dT) and latent heat storage (ML<sub>f</sub>). This is used to calculate the heat storage rates, both instantaneous and average, as follows:

$$\begin{aligned} \dot{E}_t &= \frac{E_{t+1} - E_t}{dt} \\ \dot{E}_{mean} &= \frac{E_{end} - E_{ini}}{t_m} \end{aligned} \quad (5)$$

where  $dt$  and  $t_m$  is the time step size and melting time, respectively, and  $E$  is the total energy of the PCM.

### 3.2. Initial and boundary conditions

The problem of latent heat storage in a horizontal shell-and-tube casing design can be modeled by the above set of partial differential equations (PDEs) that describe the temperature distribution in the fluid and solid domains. To solve these PDEs, it is required to specify the initial and boundary conditions for the temperature variable. The initial condition is that the whole system has a uniform temperature of  $T_{ini} = 50^\circ\text{C}$  at  $t = 0$ . The boundary conditions are that the inner tube has a constant surface temperature of  $T_w = 20^\circ\text{C}$ , and that the outer shell is fully insulated, meaning that there is no heat flux across its surface. It is also assumed that the fluid flow rate is high enough to keep the inner pipe temperature constant, so the problem can be simplified to a 2D domain. Moreover, the effect of gravity on the fluid density is assumed downward and perpendicular to the bottom surface of the inner tube.

### 3.3. Numerical scheme

CFD modeling and simulation is a reliable methodology to evaluate the performance of a proposed system

design prior to manufacturing, facilitating the confirmation or dismissal of any design modifications (Amano & Sundén, 2011). The emergence of CFD codes like ANSYS FLUENT has broadened the scope for identifying intricate attributes of flow and heat transfer in a wide variety of complex heat exchanger designs (Karar et al., 2021; Menni et al., 2021; Zandie et al., 2022) and heat transfer enhancement techniques (Darbari et al., 2020; Keshmiri et al., 2015; Mashayekhi et al., 2020; Shamsabadi et al., 2020). The ANSYS FLUENT solver, utilizing the SIMPLE scheme for pressure-velocity coupling, was employed to conduct the simulation runs in this study. The pressure correction equation was solved using the PRESTO scheme, while the momentum and energy equations were solved using the QUICK scheme. The convergence criteria for the continuity equations and velocity components were set at  $10^{-4}$ , indicating that the iterations continued until the relative differences in these quantities reached a magnitude of  $10^{-4}$ . For the energy equation, a more stringent convergence criterion of  $10^{-6}$  was applied, ensuring a higher level of accuracy in the calculations.

### 3.4. Mesh and time step analysis

In order to analyze the mesh independence of a case involving three fins with a curvature angle ( $\alpha$ ) of  $60^\circ$ , three distinct cell sizes: 0.25, 0.5, and 1 mm were selected. Additionally, three different time step sizes were considered: 0.1, 0.2, and 0.4 s. The objective was to determine the optimal grid size that ensures grid-independent solution by comparing the heat recovery rates for each case. The calculations were performed for the whole solidification process. The results, presented in Figure 3(a), indicate that the liquid-fraction evolution curves for mesh sizes of 0.25 and 0.5 mm are very similar. Consequently, a mesh size of 0.5 mm was chosen. It should be noted that the time step size used for the mesh size study was 0.2 s. Upon analyzing the time step size, it was observed that the results were highly comparable, as shown in Figure 3(b). The liquid-fraction evolution curves for time step sizes of 0.1 and 0.2 s were found to be identical. Therefore, a time step size of 0.1 s was selected for further investigations.

### 3.5. Model validation

The experimental validation of the present model is performed via the work of Al-Abidi et al. (2014), who investigated the temperature distribution of PCM during solidification in a triple-pipe heat exchanger with longitudinal fins. They used fifteen thermocouples at different radial and angular positions to cover all the regions of

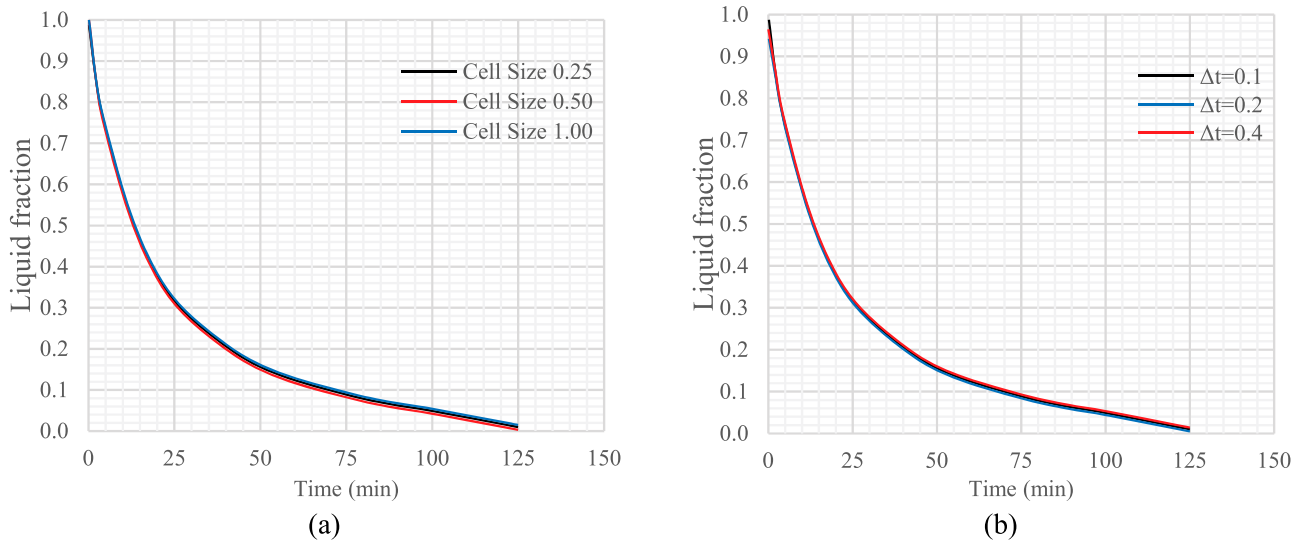


**Figure 3.** The timewise variation of liquid fraction for various sizes of (a) the mesh cell and (b) the time step for scenario 3 in Table 1.

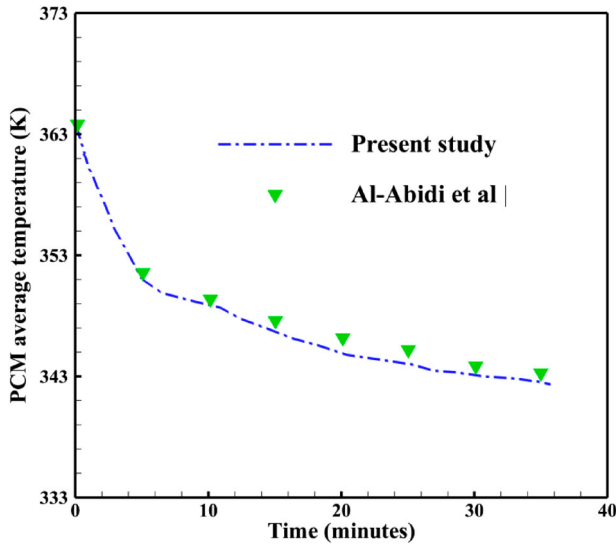


**Figure 4.** Code verification during the solidification mode using the experimental findings of Al-Abidi et al. (2014).

the PCM domain and compared them with the numerical simulations. The present study and the work of Al-Abidi et al. (2014) show a good agreement, as illustrated in Figure 4, which shows the average temperature gradient. The maximum deviation in the average temperature of PCM between the two works is less than 1.5 °C. This implies that the present model can accurately predict the discharging process compared to the experimental results.

## 4. Results and discussion

### 4.1. Effect of varying the fin curvature angle

The introduction of arc-shaped fins induces fluid behavior and improves heat transport rate during the energy

discharge mode (i.e. solidification), and hence positively affects the solidifying front evolution and temperature distribution. Figure 5 compares the phase evolution contours on the left and temperature contours on the right for the case of a single arc-shaped fin with a curvature angle ranging from 60° to 180° over discharge durations of 300, 1800, 5400, and 9000 s. The solidified part of PCM is observed to gradually witness the growth of solidifying fronts, which are distinguished by almost homogeneous, light-green semicircles. These semicircles have similarities in the upright direction among the studied cases of arc-shaped fins. It is clear from analyzing the figure that by employing a larger curvature angle, the arc-shaped fins motivate bigger solidifying layers (blue areas) to form in the interstices between and around the fin ligaments. However, during the early duration ( $t = 300$  s), the relationship between the varying curvature angle and the increase in the solidifying layers is still not noticeable at this point. The reason for this observation pertains to the fact that during this earlier time stage, only thin layers of solidification are able to form. As time passes further and closer to the point where it reaches ( $t = 1800$  s), the shapes of the solidifying fronts begin to distort increasingly, and larger solidifying layers become able to form. This is especially obvious when cases with smaller curvature angles of fins, such as those in the case of ( $\alpha = 60^\circ$ ), are compared to those with larger curvature angles of fins, such as in the cases of ( $\alpha = 120^\circ$  or  $180^\circ$ ). The slower heat recovery rates at the cooling walls are likely to blame for this phenomenon as decreasing the curvature angle results in reducing the area for heat communication with the cooling walls. When examining the same contour maps, it is possible to recognize that the area of solidifying strata (blue zones) appears to be progressively



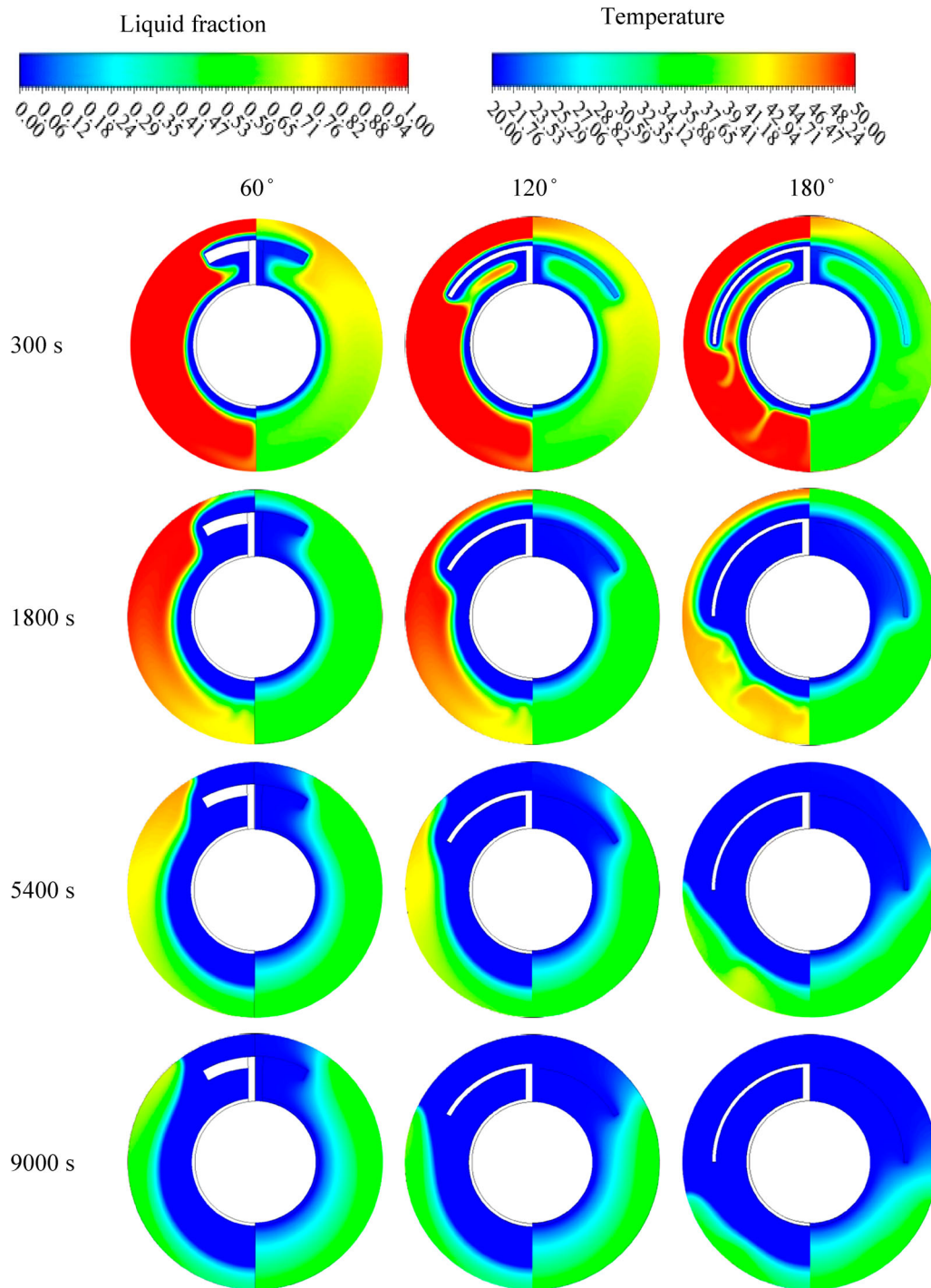


**Figure 5.** Contour maps for solidifying front evolution (left side) and temperature distribution (right side) for fin curvature angles ( $\alpha = 60, 120$  and  $180^\circ$ ) during the solidification mode.

increasing toward the bottom over the course of the 5400s timeframe. This can be recognized to take place in a downward direction. The reason for such a phenomenon would be the point that convection mode of the heat transfer process plays a more significant role in the uppermost sections of the domain than it does in the lowermost sections of the domain (Darzi et al., 2016), (Mahdi et al.,

2018), and (Nie et al., 2020). This also justifies why arc-shaped fins with higher curvature angles ( $\alpha = 120$  and  $180^\circ$ ) have the benefit of allowing for larger heat dispersion from PCM layers that be away from cooling walls. Such fin arrays also have the advantage of promoting faster expansion of the solidifying layers during the subsequent duration of solidification (i.e.  $t = 9000$  s). This is

the major advantage associated with arc-shaped fins with higher curvature angles. In fact, more heat is conducted by the fin ligaments to the PCM layers, since more of the fin's surface area is exposed as the curvature increases to  $180^\circ$ . Meanwhile, the presence of such a long fin curvature limits the contribution of natural convection in the top section of the PCM domain due to the higher flow resistance produced as the curvature angle increases. This can be observed when comparing the isotherm distribution in the top section of the domain when the curvature angle increases from  $60^\circ$  to  $180^\circ$ . The presence of lower-curvature arc-shaped fins enhances the impact of natural convection as the temperature distribution contours become more nonuniform, which is an evidence for a stronger role of natural convection, particularly in the later stages of solidification. Therefore, increasing the fin curvature has a detrimental impact on the natural convection that occurs in the upper zones of the PCM domain, but it has a beneficial impact on the thermal conduction that predominates the other zones of the domain. This can be attributed to the unique flow-aiding configuration that arc-shaped fins have, which makes them superior to other configurations when it comes to promoting heat transfer through conduction.

The timewise progression of the solid PCM fraction and the average temperature profiles were also investigated to provide more insight into the potential of arc-shaped fins for energy discharge intensification of PCM in the shell-and-tube confinement system. The variation in the solid fraction over time is depicted in Figure 6 for three different cases of fin curvature angle ( $\alpha = 60, 120$ , and  $180^\circ$ ). It is clear that the rates of solidification in the early period are almost the same across all three cases. As the process of solidification continues, the fin structure that has a greater curvature angle has better performing solidifying behavior. So, employing arc-shaped fins with a higher curvature angle improves heat transport, which ultimately results in a higher solidification rate throughout the system. According to this figure, the PCM with the greatest fin curvature solidifies entirely in about 180 min, which is a significant amount of time less than the other instances. This is because arc-shaped fins with a curvature angle of  $180^\circ$  hold a larger heat-exchanging area, which helps in the earlier solidification completion throughout the PCM unit. In light of this, the case with arc-shaped fins of a large curvature angle of  $180^\circ$  is found to have the best potential for solidification improvement as compared to the other cases of lower curvature angle ( $\alpha = 60^\circ$  and  $120^\circ$ ). Figure 7 illustrates the variation in the mean temperature profile encountered by the PCM during the solidification phase for the three distinct angles of arc-shaped fins that are being examined. The figure illustrates that the PCM attains its minimum

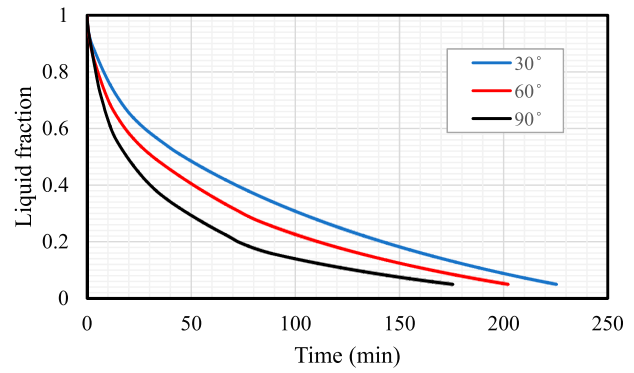


**Figure 6.** Timewise variation of liquid fraction for fin curvature angles ( $\alpha = 60, 120$  and  $180^\circ$ ) during the solidification mode.

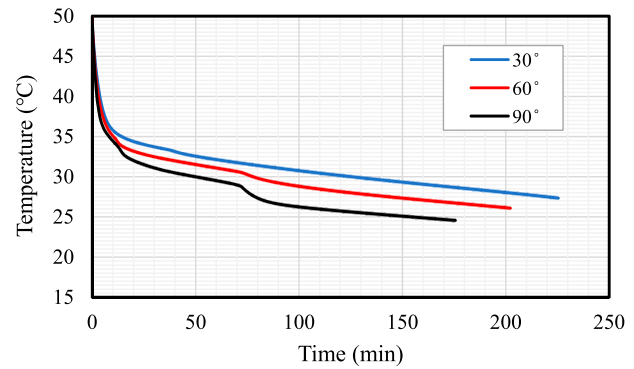


**Figure 7.** Timewise variation of average PCM temperature for fin curvature angles ( $\alpha = 60, 120$  and  $180^\circ$ ) during the solidification mode.

temperature in a comparatively shorter duration when the curvature angle is configured to  $180^\circ$  in contrast to the other two curvature angles. Predictions show that using arc-shaped fins with wider angles of curvature can drastically shorten the time it takes to reach the maximum solidification temperature. So, the implementation of such fins of wider curvature can remarkably expedite the heat transfer process from the thermally active walls toward the adjacent PCM layers. This, in turn, results in an accelerated solidifying rate of the PCM. The degree of curvature angle has been found to have a direct impact on the rate of solidification, with an increase in the curvature angle from  $60^\circ$  to  $180^\circ$  leading to earlier completion of the PCM solidification process, as alluded to earlier in this section. The data pertaining to the solidifying time and heat recovery rate for all cases examined in this section have been consolidated in Figure 8 which show that the solidifying times were recorded at 225.4, 202.2, and 175.6 min. The heat recovery rates were recorded at 21.5, 24.3, and 28.4 Watts for cases with fins of curvature angles 60, 120, and  $180^\circ$ , respectively. The

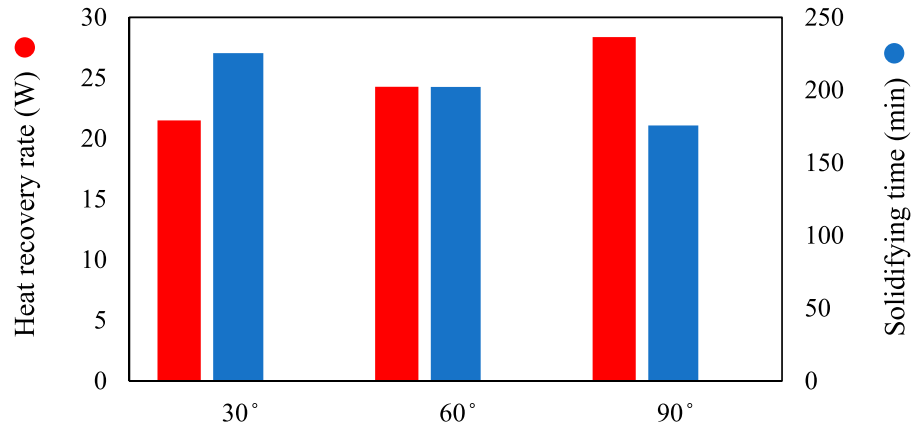


**Figure 8.** Total solidifying times and average recovery rates for fin curvature angles ( $\alpha = 60^\circ, 120^\circ$  and  $180^\circ$ ) during the solidification mode.

findings suggest that augmenting the curvature of arc-shaped fins from 60 to 120 and 180° would yield solidifying time savings of about 10.3% and 22.1%, respectively, while also improving the heat recovery rates by about 12.9% and 32.0%.

#### 4.2. Effect of varying the spacing of fin base

After identifying the ideal case for fin curvature angle (i.e.  $\alpha = 180^\circ$ ), this section examines the impact of varying the placement of arc-shaped fin from the active wall to find the best fin spacing for enhanced solidifying performance. Figure 9 compares the contour lines of liquid fraction (left) and PCM temperature (right) for discharge periods of 300, 1800, 5400, and 9000 s for three different lengths of fin base ( $\delta = 5, 10$ , and 15 mm). The maps for liquid-fraction evolution show that employing lower lengths for the fin base, larger solidifying layers (blue regions) are developed between and around the fin zones during the timeframes of 1800 and 5400 s. This is particularly true for smaller values like  $\delta = 5$  or 10 mm. During the last time period ( $t = 9000$  s), as shown by the contour maps in Figure 9, the size of the solidifying layers (blue zones) seems to be slowly diminishing toward the bottom. One possible explanation for this behavior of solid PCM is that convection, which provides an extra sink of heat removal from PCM, is more prevalent at the higher areas of the domain. So, the length of fin base can be decreased to improve the capability of natural convection currents to remove further heat from PCM components near the thermally active wall. Therefore, arc-shaped fin arrays are more favorable in terms of improving the heat removal rates during the solidification phase if the base spacing increases. A quick glance at the isotherm maps signifies that the size of the isotherm layer with temperatures below 25 °C (shown as blue patches) gradually increases throughout the domain, notably at the larger

spacings of  $\delta = 10$  and 15 mm. In the later discharge periods ( $t > 5400$ s), the cooling impact on PCM solidifying behavior increases, causing the solidifying layer to grow in size and finally cover the whole domain. This is because more buoyancy-driven flows could be formed between the fin ligaments if the base length of arc-shaped fins increases, leading to more efficient natural convection heat transfer. Meanwhile, a longer fin base means more surface area of fins is involved in the heat communication with PCM components, allowing the fin ligaments to carry more heat from these layers. This justifies why there is a stronger nonuniformity of isotherm distributions in cases with longer fin base, such as the case of  $\delta = 15$  mm, over the final period (i.e.  $t = 9000$ s). At smaller spacings of fin base, and notably in the domain's upper sections, the isotherm's discoloration suggests that convection contributes more than conduction. Because of the effective involvement of convection in these regions, it seems that isotherms gradually became more regular in shape and behavior throughout the last periods, especially at lower spacings of the fin base. In conclusion, the natural convection in the top zones of the PCM domain is positively affected by increasing the spacing of the fin base, while thermal conduction continues to be the predominating mode in the other zones.

Figure 10 shows the progression of liquid-fraction profile over time for three distinct cases of the spacing of fin base ( $\delta = 5, 10$ , and 15 mm). It is evident that the solidifying rates in all three cases do not show significant differences during the early stages of solidification. However, the fin structure with a larger spacing has better performing solidifying behavior as the solidification process progresses. As a consequence, using arc-shaped fins with a larger spacing from the active wall enhances heat transfer, which eventually increases the PCM's solidification rate. The performance curves in Figure 10 show

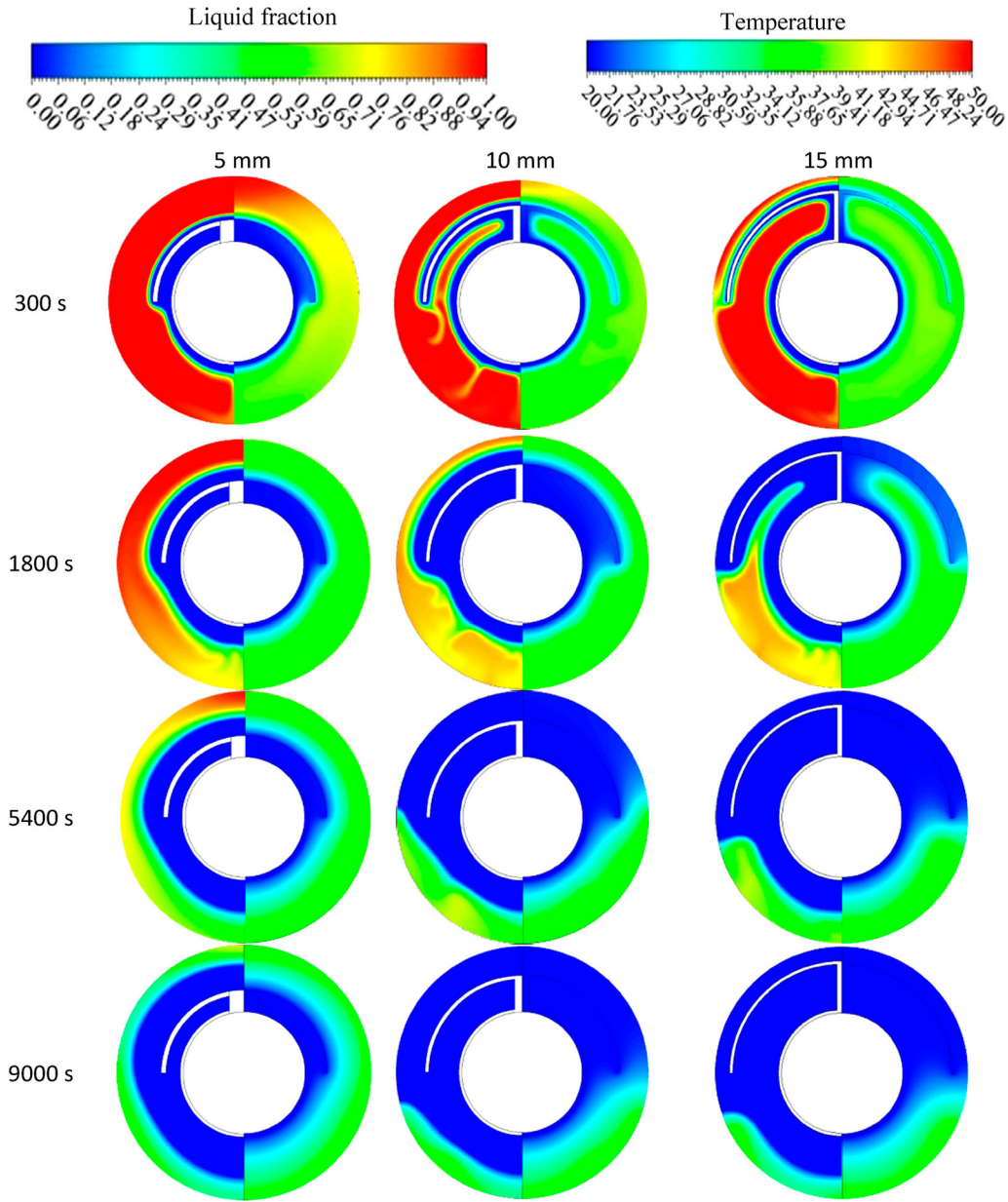


**Figure 9.** Contour maps for solidifying front evolution (left side) and temperature distribution (right side) for the spacing of fin base ( $\delta = 5, 10$  and  $15$  mm) during the solidification mode.

that the PCM with the largest fin spacing ( $\delta = 15$  mm) solidifies completely in roughly 165 min, which is much less time than the other cases. This is due to the bigger heat-exchanging area held by arc-shaped fins with a 15-mm fin spacing, which aids in the PCM quicker solidification completion. This means that, when compared to the two cases with lesser fin spacings ( $\delta = 5$  and  $10$  mm), the case with arc-shaped fins of a high spacing from the active wall has the most potential for improving solidification. Figure 11 depicts the progression of the average temperature profile that the PCM experienced during the solidification phase for the three

different arc-shaped fin spacings that are being investigated. The figure shows that, in comparison to the other two spacings, the PCM reaches its lowest temperature in a considerably shorter amount of time when the fin spacing is adjusted to ( $\delta = 15$  mm). The time it takes to achieve the minimum solidification temperature ( $T = 25^\circ\text{C}$ ) is significantly sped up by implementing arc-shaped fins with greater spacings from the active wall. Therefore, using fins with larger spacing can significantly speed up the removal of heat from neighboring PCM layers to the thermally active walls. The nearby PCM layers then begin to solidify more quickly as a consequence of this. This



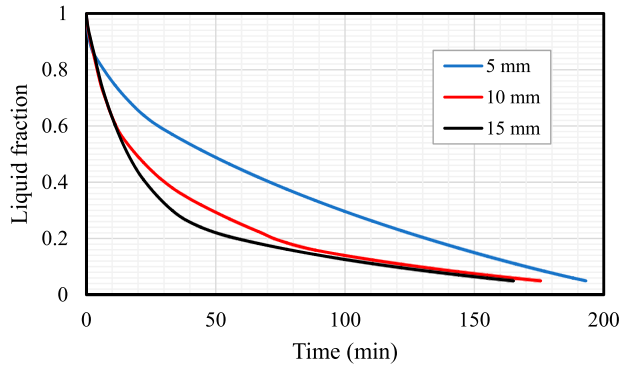


**Figure 10.** Timewise variation of liquid fraction for the spacing of fin base ( $\delta = 5, 10$  and  $15$  mm) during the solidification mode.

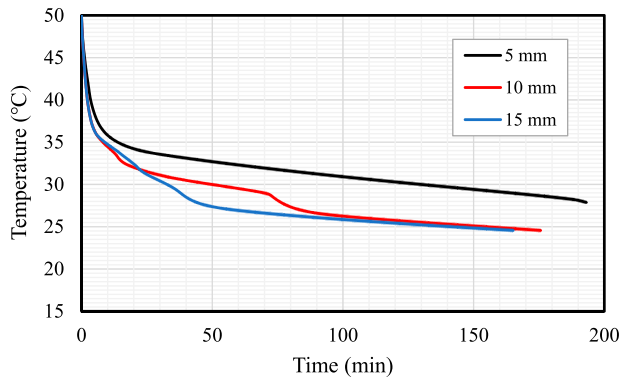


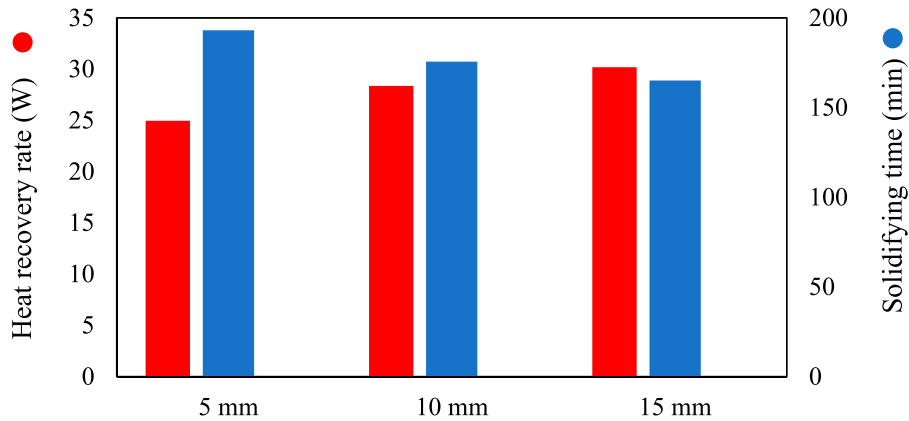
**Figure 11.** Timewise variation of average PCM temperature for the spacing of fin base ( $\delta = 5, 10$  and  $15$  mm) during the solidification mode.

implies that the rate of solidification is directly affected by varying the fin spacing from the active wall, with an increase in fin spacing from 5 to 15 mm resulting in an earlier completion of the PCM solidification process. Figure 12 provides the data on the heat recovery rate

and solidifying time for each of the three cases considered in this section. The data collected shows that for cases with fins at 5, 10, and 15 mm of spacing from the active wall, the solidification periods were recorded at 193.1, 175.6, and 165.1 min, while the heat recovery rates were recorded at 24.96, 28.37, and 30.17 Watts, respectively. According to these numbers, increasing the spacing of arc-shaped fin from 5 to 10 or 15 mm will result in solidifying time reductions of around 9.1% and 14.5%, respectively, while simultaneously increasing heat recovery rates by about 13.7% and 20.9%.

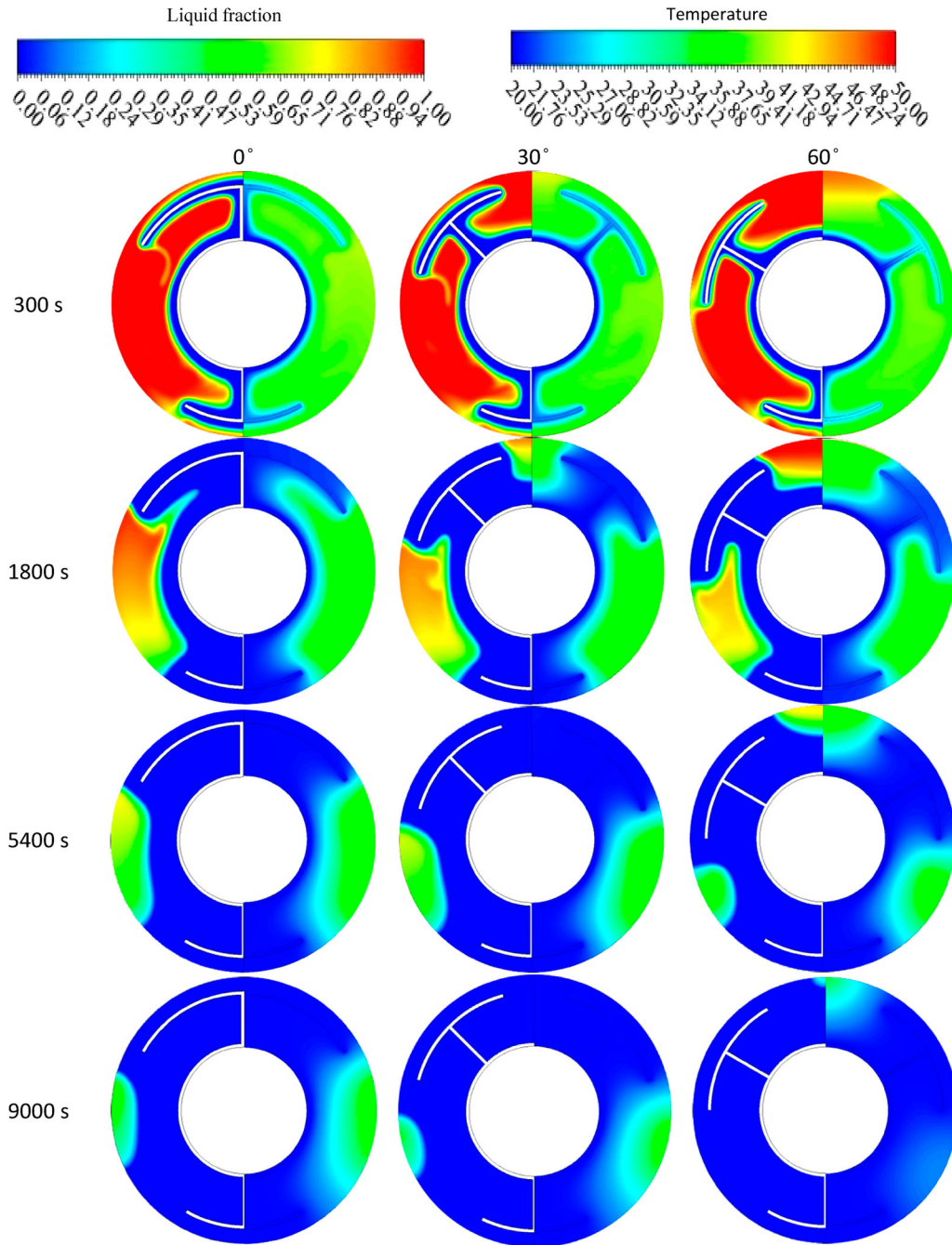
#### 4.3. Effect of varying the joining angle between top fins

Figure 13 compares the contour lines for PCM liquid fraction (left) and average PCM temperature (right) for arc-shaped fins with joining angles of ( $\beta = 0^\circ, 30^\circ$ , and  $60^\circ$ ) between the upper fins throughout the discharge periods of 300, 1800, 5400, and 9000 s. The figure illustrates that increasing the angle between the upper fins from 0 to  $60^\circ$  allows for bigger solidifying layers (blue areas) to form in the interstices around the fin ligaments during the course of solidification. This is owing to the fact that the PCM's ability to release is boosted by the integration of arc-shaped fins with an appropriate connecting angle. Over the course of the first 1800 s, the region occupied by the solidifying layers (the blue zones) progressively expands inside the top half of the PCM domain. When the joining angle is expanded to  $60^\circ$ , the solidifying front moves more quickly near the fin ligaments. This can be attributed to the substantial enhancement of heat release towards the thermally active walls. Notably, the increase in space between the side fins, due to a larger joining angle, leads to a quicker buoyancy-driven flow of the liquid PCM. This in turn



**Figure 12.** Total solidifying times and average recovery rates for the spacing of fin base ( $\delta = 5, 10$  and  $15$  mm) during the solidification mode.





**Figure 13.** Contour maps for solidifying front evolution (left side) and temperature distribution (right side) for the joining angle between upper fins ( $\beta = 0, 30$  and  $60^\circ$ ) during the solidification mode.

helps the solidifying front gains stronger potential to move when the joining angle of arc-shaped fins expands from  $30^\circ$  to  $60^\circ$  during the later durations of 5400s and 9000s. This enables the solidification to invade the whole upper half of the PCM domain. This, in turn, brings positive impact to the contribution of convection to the overall solidification process. This justifies why there is more discoloration of isotherms in cases with wider joining angle, such as the case of  $\beta = 60^\circ$ , throughout the

prefinal period of 5400 s. The discoloration of isotherms implies that natural convection plays a more significant role in cases of wider fin angles, especially in the upper half of the domain. However, isotherms gradually move from discoloration to become more regular in shape in major part of the PCM domain during the last period of 9000 s, indicating that thermal conduction continues to be the predominating mode in almost the whole PCM domain.

The average liquid-fraction variation over time is shown in Figure 14 for the three cases of the fin joining angle ( $\beta = 0, 30$ , and  $60^\circ$ ). The solidification rates across all three cases exhibit not much significant difference throughout the entire solidification period. Nevertheless, the fin structure with a larger joining angle between the upper fins has better performing solidification behavior during the whole process. It can be observed from Figure 14 that the PCM with larger degree of the upper fin joining angle ( $\beta = 60^\circ$ ) attains complete solidification in about 100 min, which is considerably shorter than the solidifying time for the other cases. This phenomenon can be attributed to the fact that any increase in the angle between upper fin ligaments will cause a corresponding increase in the available space for convective currents to move in the upper half of the PCM domain. This, in turn, results in a higher rate of heat removal across the involved PCM layers. In this regard, the results signify that augmenting the angle between the upper fin segments results in an improved flow-assisting environment for arc-shaped fin arrays, thereby rendering them more beneficial for intensifying the heat transfer rates through natural convection. The variations in mean temperature experienced by the PCM during solidification for the three cases of the angle joining the upper arc-shaped fins are illustrated in Figure 15. The presented figure indicates that the PCM attains its minimum temperature at a significantly faster rate when the upper fin joining angle is set to its highest value ( $\beta = 60^\circ$ ), as opposed to the other two joining angles. The time it takes to reach the minimal solidifying temperature ( $T = 25^\circ\text{C}$ ) is substantially less when a greater joining angle between upper fins is applied. So, employing arc-shaped fins that feature a greater joining angle can expedite the dissipation of heat from the involved PCM layers towards the thermally active walls. The solidification rate is impacted by alterations in the fin joining angle, whereby an increase

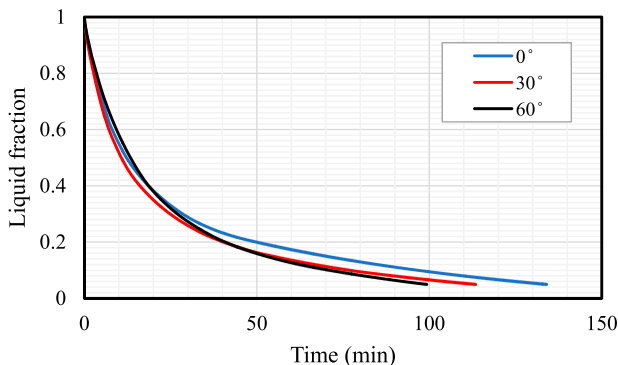


**Figure 14.** Timewise variation of liquid fraction for the joining angle between upper fins ( $\beta = 0, 30$  and  $60^\circ$ ) during the solidification mode.

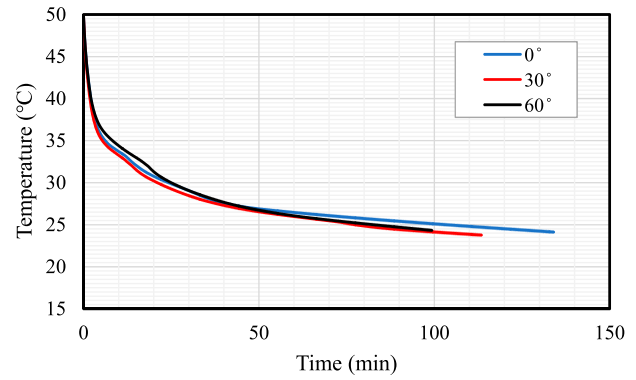


**Figure 15.** Timewise variation of average PCM temperature for the joining angle between upper fins ( $\beta = 0, 30$  and  $60^\circ$ ) during the solidification mode.

in the angle from  $0$  to  $60^\circ$  leads to an earlier completion of PCM solidification. The data pertaining to the heat recovery rate and solidifying time for each of the three cases discussed in this section is presented in Figure 16. The collected data indicates that the solidification periods and heat recovery rates were measured for cases with joining angles of  $0, 30$ , and  $60^\circ$  between the upper fins. The solidification periods were found to be 134, 113.4, and 99.3 min, respectively, while the corresponding heat recovery rates were recorded at 37.33, 44.27, and 50.30 Watts. Based on the data presented, it can be inferred that augmenting the joining angle between the upper arc-shaped fins from  $0^\circ$  to  $30^\circ$  or  $60^\circ$  would lead to a decrease in solidifying time by approximately 15.4% and 25.9%, respectively. Additionally, this alteration would result in an increase in heat recovery rates by roughly 18.6% and 34.7%.

#### 4.4. Effect of varying the joining angle between bottom fins

After identifying the best values for fin curvature angle, spacing of fin base, and the angle between top fins, this section explores the effect of varying the angle between bottom fins to identify where the arc-shaped fins should be installed for greater enhancement rates of solidification. It is worthy to mention that the selection of the angle between the bottom fins as a design parameter is primarily driven by its direct impact on local heat release within the PCM domain. The lower sections of PCM domain, which predominated by conduction for heat removal, can substantially benefit from modifications in the fin angle. Therefore, adjusting the angle between the bottom fins can serve to optimize the fin configuration, thereby enhancing the rate of heat removal across the entire PCM domain. Conversely, the upper sections of the domain, where natural convection is effective,

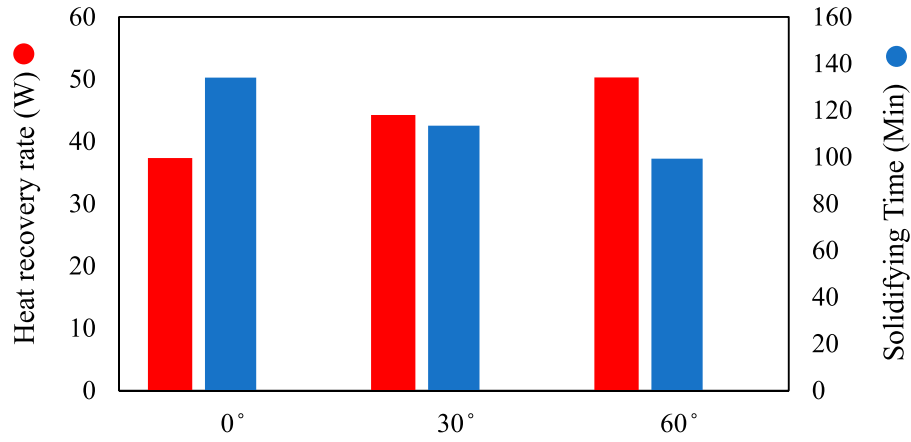


**Figure 16.** Total solidifying times and average recovery rates for the joining angle between upper fins ( $\beta = 0, 30$  and  $60^\circ$ ) during the solidification mode.

necessitate adjustments in the angle between the top fins. Such alterations can similarly optimize the distribution of fins and, as a result, promote the heat release across the PCM domain.

Figure 17 illustrates the contour lines for liquid fraction (on the left) and PCM temperature (on the right) for arc-shaped fins with joining angles of ( $\gamma = 30^\circ, 60^\circ$ , and  $120^\circ$ ) between the bottom fins during the discharge durations of 300, 1800, 5400, and 9000 s. The illustration shows that increasing the angle between the bottom fins from  $30^\circ$  to  $120^\circ$  has a detrimental effect on the size of the solidifying layers (blue zones) that grow between and around the fin sections as the solidification process goes on. During the first 1800 s of the process, the size of PCM layer that is solidifying (the blue zones) gradually extends upward toward the upper half of the domain. However, the presence of fins with wider angles at the bottom will negatively affect the good role played by convection in the lower half of the domain. The reason behind is that the space available for the move of convective currents decreases as the bottom fins with wider angle are applied. In light of this, the capability for the PCM to solidify becomes lower when the connecting angle of the arc-shaped fins grows from  $30^\circ$  to  $120^\circ$  in the late durations of 5400 and 9000 s. Because of this, the solidification may now invade the whole of the bottom half of the PCM domain in cases of  $\gamma = 30$  and  $60^\circ$ . Meanwhile, increasing the bottom fin angle to  $\gamma = 120^\circ$  will result in a lower flow of liquid PCM that is propelled upward by buoyancy due to the increased flow suppression by wider-angle fins. Because of this, the contribution that convection makes to the overall heat removal process will now have a detrimental influence. This explains why there is a lower degree of discoloration of isotherms in cases that include a broader joining angle, such as the case of  $\gamma = 120^\circ$ , over the whole of the prefinal phase that lasts for 5400 s. This less discoloration of the isotherm demonstrates that the

contribution of convection is less obvious with broader fin angles, which is especially true in the lower half of the domain. Isotherms, on the other hand, migrate progressively from discoloration to becoming more regular in form throughout the majority of the PCM domain over the final period of 9000 s, which indicates that heat conduction continues to be the predominating mode in the entire PCM domain.

The impact of varying the average liquid-fraction over time on the solidification behavior of PCM is shown in Figure 18 for the three cases of the bottom fin joining angle ( $\gamma = 30, 60$ , and  $120^\circ$ ). The results show that the solidification rates across all three cases ( $\gamma = 30, 60$ , and  $120^\circ$ ) exhibit not much significant difference throughout the entire solidification period. However, the fin structure with small joining angle between the bottom fins (i.e.  $\gamma = 30$  and  $60^\circ$ ) have better performing solidification behavior during the whole process. This is due to the fact that a severe increase in the angle between bottom fin ligaments will pose higher resistance for convective currents moving in the bottom half of the PCM domain, resulting in a lower rate of heat removal across the involved PCM layers. The results from Figure 19 show that the PCM attains its minimum temperature at a significantly faster rate when the bottom fin joining angle is set to its lowest value ( $\gamma = 30^\circ$ ), compared to the other two joining angles. The time it takes to reach the minimal solidifying temperature ( $T = 25^\circ\text{C}$ ) is significantly smaller when a lower value for the joining angle between bottom fins is applied. Therefore, employing arc-shaped fins that feature a lower joining angle can expedite the dissipation of heat from the involved PCM layers towards the thermally active walls. The data pertaining to the heat recovery rate and solidifying time for each of the three cases discussed in this section is presented in Figure 20. The collected data indicates that reducing the joining angle between the bottom arc-shaped fins from  $120^\circ$  to  $60^\circ$  and  $30^\circ$

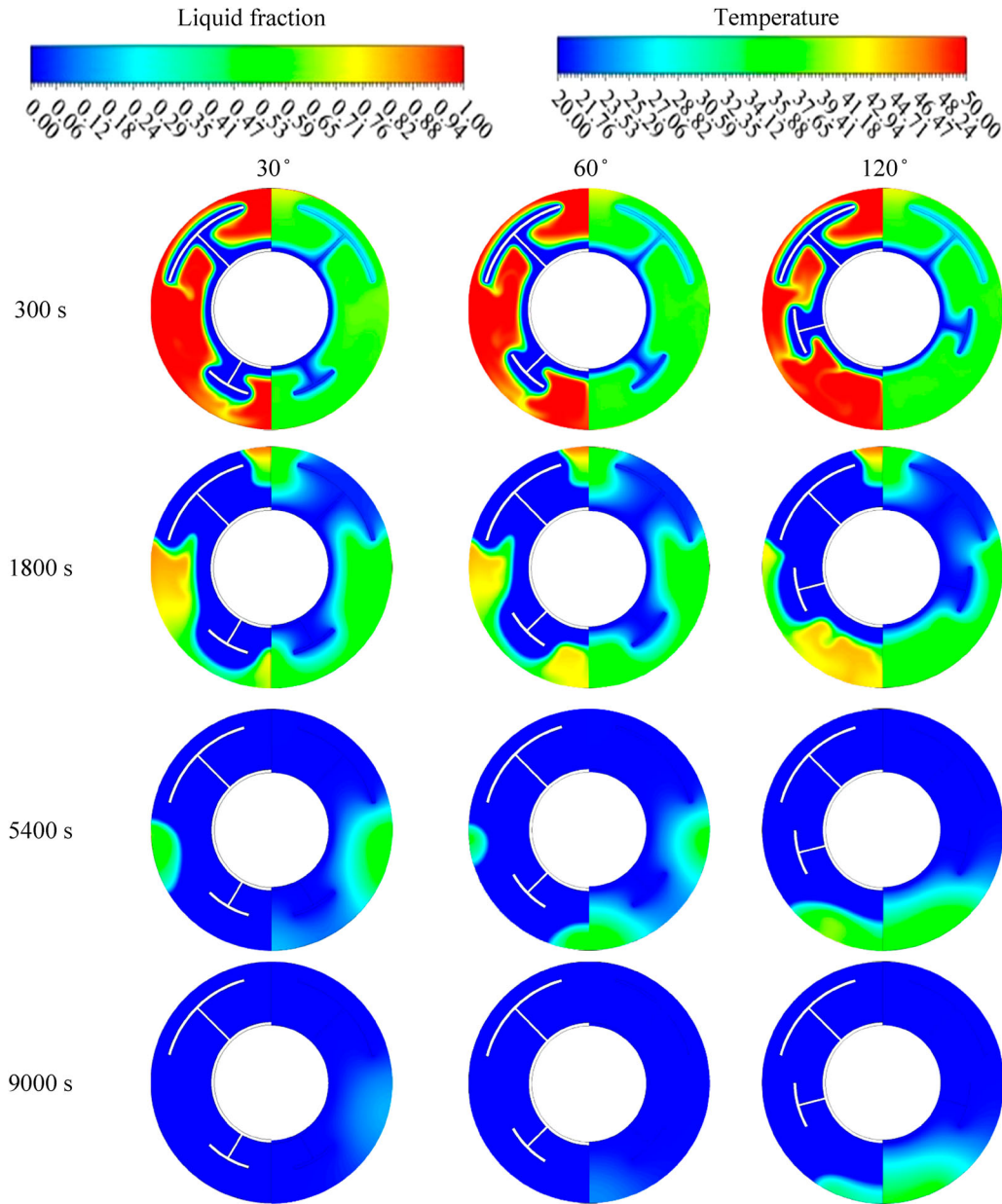


**Figure 17.** Contour maps for solidifying front evolution (left side) and temperature distribution (right side) for the bottom joining fin angle ( $\gamma = 30^\circ, 60^\circ$  and  $120^\circ$ ) during the solidification mode.

will reduce the solidifying time from 116.1 min to 79.8, and 82.2 min, respectively, while the corresponding heat recovery rates will increase from 43.5 Watts to 62.6, and 60.9 Watts. Therefore, reducing the joining angle between the bottom arc-shaped fins from  $120^\circ$  to  $60^\circ$  or  $30^\circ$  would lead to a decrease in solidifying time by approximately 31.3% and 29.2%, respectively. Additionally, this alteration would result in an increase in heat recovery rates by roughly 44.1% and 40.1%, respectively. In conclusion, the results suggest that augmenting the angle between the bottom fin segments results in a negative flow-assisting environment for arc-shaped fin arrays, thereby rendering

them less beneficial for intensifying the heat transfer rates through natural convection. Therefore, choosing a proper joining angle between the bottom fins can significantly improve the solidification behavior of PCM and enhance heat recovery rates.

#### **4.5. Comparison of the optimum case with the case without fins, as well as conventional longitudinal fins**

The preceding analysis investigated multiple comparisons to identify the optimum configuration for arc-shaped fins, employing various design parameters.



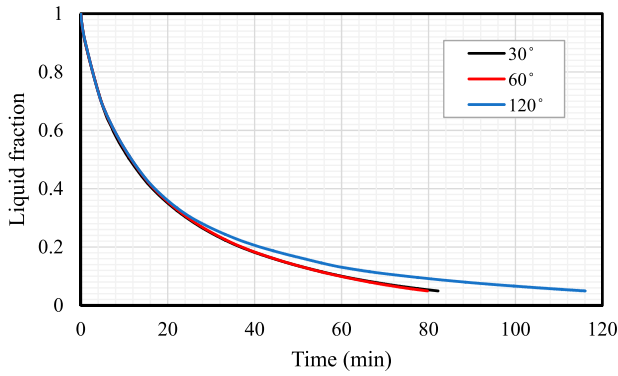


**Figure 18.** Timewise variation of liquid fraction for the joining angle between bottom fins ( $\gamma = 30, 60$  and  $120^\circ$ ) during the solidification mode.

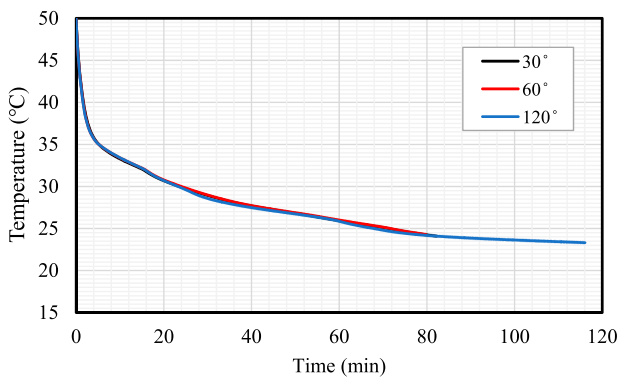


**Figure 19.** Timewise variation of average PCM temperature for the joining angle between bottom fins ( $\gamma = 30, 60$  and  $120^\circ$ ) during the solidification mode.

The optimal parameters that were determined so far: the curvature angle of the fins ( $\alpha = 180^\circ$ ), the base-spacing of the fins ( $\delta = 15$  mm), the angle of conjunction for the upper fins ( $\beta = 30^\circ$ ), and the joining angle for

the bottom fins ( $\gamma = 60^\circ$ ). This section presents additional comparisons to further confirm the outperforming potential of arc-shaped fins for solidification enhancement. The comparison of liquid-fraction contours and temperature distribution for three distinct fin configurations, namely arc-shaped fins, no fins, and + -shaped fins, is presented in Figure 21. For a meaningful comparison, the cases studied are designed to maintain a constant volume for the fin sections. The time variation of liquid-fraction contours is depicted on the right, while the temperature distribution is shown on the left. The analysis of the solidifying front, as illustrated by the light green line, reveals a discernible augmentation in the size of the solidifying layer (blue zone) over time, which is suggestive of accelerated solidification with arc-shaped fins. The observed phenomenon can be ascribed to the advantageous impact of conduction, particularly in the lower portion of the PCM system. In this region, arc-shaped fins exhibit a superior solidification rate compared to their counterparts, thereby promoting an accelerated solidification mechanism. Moreover, the flow-enhancing structure of arc-shaped fins amplifies the role of convection in the heat removal process, outperforming alternative fin configurations. +shaped fins exhibit increased flow resistance as a result of their structural composition, thereby limiting the overall impact of convection on the solidification progression. Therefore, arc-shaped fins offer significant advantages over other configurations in terms of improving solidifying front movement and liquid-fraction evolution. Figure 22 also reveals that as time progresses from 1800 to 9000 s, the isotherms become more deformed, particularly in the case of arc-shaped fins when compared to other configurations. The observed phenomenon can be ascribed to the advantageous role of natural convection as an additional source

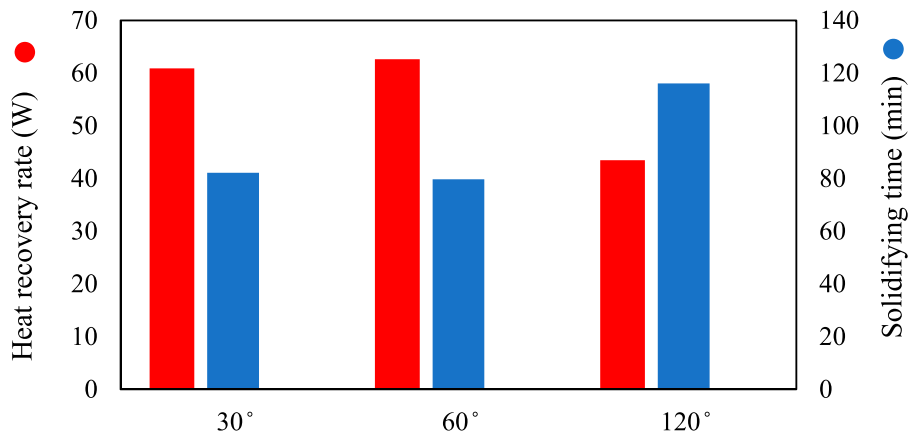


**Figure 20.** Total solidifying times and average recovery rates for the joining angle between bottom fins ( $\gamma = 30, 60$  and  $120^\circ$ ) during the solidification mode.



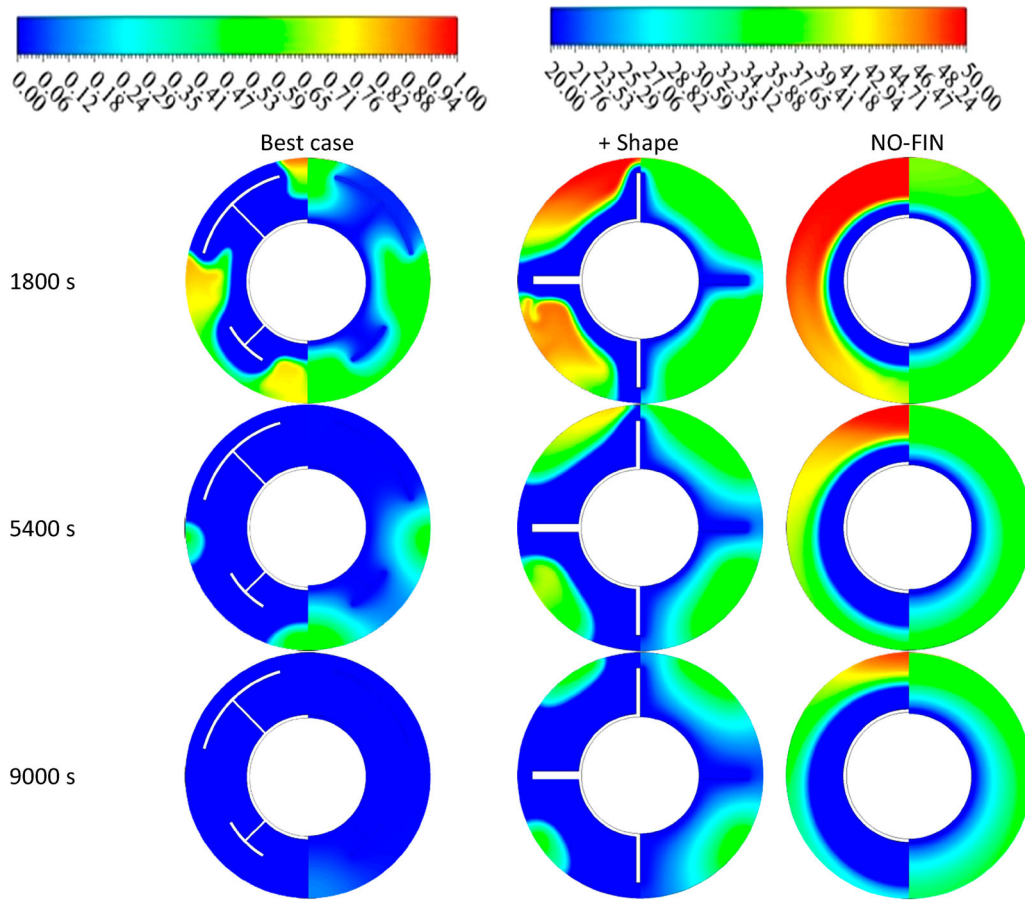


**Figure 21.** Contour maps for solidifying front evolution (left side) and temperature distribution (right side) for different fin configurations.

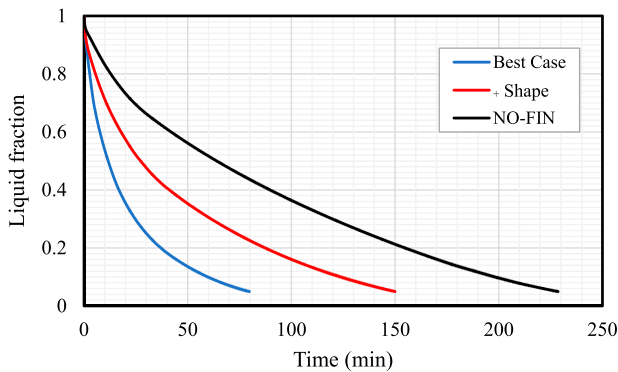


**Figure 22.** Average variation of PCM temperature for different fin configurations.

for heat removal, which is made possible by the configuration of arc-shaped fins. So, arc-shaped fins facilitate improved heat removal process more efficiently than other fin configurations, leading to accelerated solidification in the PCM domain.

Figures 22 and 23 depict the average liquid-fraction profile and PCM temperature behavior over time for the three cases of arc-shaped fins, no fins, and + -shaped fins.

The profile of liquid fraction denotes the proportion of PCM that remains in a liquid state at a specific time and position. The average temperature is determined by calculating the arithmetic mean of the temperatures at various points within the PCM domain. The results depicted in Figure 22 indicate that the PCM with arc-shaped fins attains complete solidification within approximately 80 min, exhibiting a significantly quicker solidification rate than the other fin configuration. This is due to the fact that the curved structure of arc-shaped fins follows the direction of the fluid flow of PCM and reduces the flow resistance as compared to the other fin configuration. The data from Figure 23 indicates that the arc-shaped fins case results in a comparatively shorter time for the PCM to attain its minimum temperature, as compared to the other two cases. The minimum temperature refers to the lowest temperature achievable by the PCM during the process of solidification. It can be inferred that the utilization of an arc-shaped fin possessing optimal geometrical parameters, including fin height, fin curvature, and angle connecting two fins, can lead to a noteworthy reduction in the duration needed to attain the minimum solidification temperature.

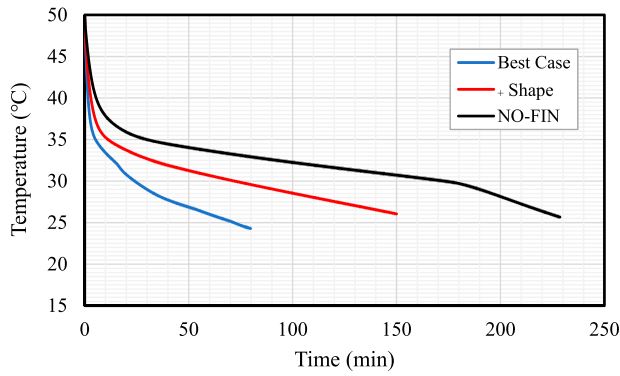


**Figure 23.** Average variation of PCM temperature for different fin configurations.

Figure 24 summarizes the data for the variation of heat recovery rate and solidifying time for three cases of arc-shaped fin arrays with different fin configuration. The data indicates that the application of arc-shaped fins has a significant impact on the solidification performance of PCM. With the use of + -shaped fins and arc-shaped fins, the solidifying time of PCM decreases from 228.6 min to 149.9 and 79.8 min, respectively. This means that the PCM can release more thermal energy in a shorter time span by about 34.4% in case of + -shaped fins, and by about 65.1% in case of arc-shaped fins compared to the case of no fins. Similarly, the heat recovery rate increases from 21.6 Watts to 32.7 and 62.6 Watts, respectively. This means that the arc-shaped fin arrays can release faster rate of thermal energy to the HTF by 190.5% compared to the case of no fins.

Based on the present findings, selecting an optimized configuration of arc-shaped fins can lead to noteworthy improvements in the solidifying time and heat recovery rates in PCM systems. In the pursuit of a sustainable future, thermal energy storage with PCMs is deemed to play a critical role as the future of TES technologies is

intrinsically tied to the ongoing evolution and increased penetration of renewable energy solutions. TES systems can serve to bridge the gap between renewable energy supply and demand, accommodating the intermittent nature of sources such as solar by storing excess energy during periods of high production and releasing it when needed. Furthermore, advances in materials science and engineering are anticipated to lead to the development of more efficient, reliable, and cost-effective TES systems. Novel PCMs and advanced system designs are likely to enhance the energy storage density, further increasing their viability for various applications.

In summary, the findings of this study suggest that adopting an optimal configuration of arc-shaped fins contributes significantly to the enhancement of solidifying behavior and heat recovery rates in PCM systems. With the growing focus on sustainable energy solutions at a global level, TES systems with PCMs are anticipated to have a significant impact. This is due to the inherent connection between the advancement of TES technologies and the wider adoption of renewable energy solutions. Hence, these technologies are effectively positioned to mitigate the mismatch between renewable energy supply and demand. Moreover, it is expected that progress in the field of materials science and engineering will result in advanced TES systems that are characterized by enhanced efficiency, reliability, and cost-effectiveness. In this context, novel PCMs and advanced system designs are likely to enhance the energy storage density, further increasing their viability for broader landscape of sustainable energy storage.

## 5. Conclusions

This article discusses the potential of arc-shaped fins to address the thermal response limitations of PCMs during the discharging phase in the horizontal shell-and-tube

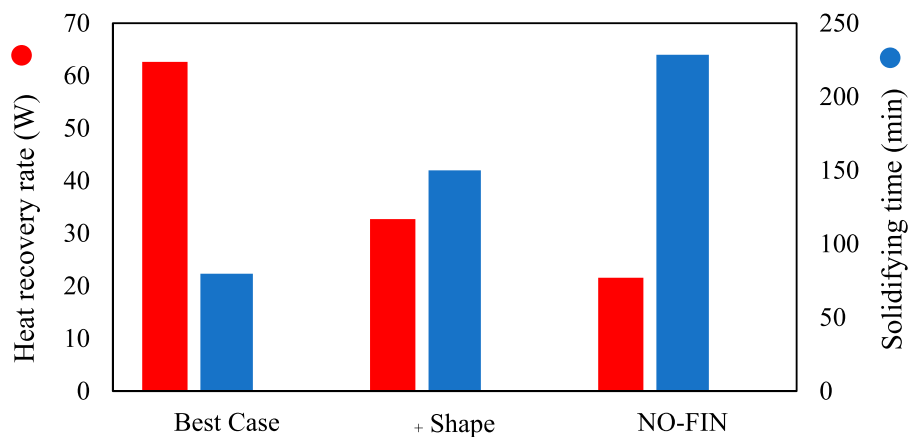


**Figure 24.** Total solidifying times and average recovery rates for different fin configurations.

storage system. A series of computational studies are conducted to explore the effects of several arc-shaped fin geometric parameters, including the fin curvature angle, the spacing of the fin base, and the nonuniform angle between fins in the top and bottom regions of the PCM domain. The main findings of this study are as follows:

- (1) Employing arc-shaped fins with a higher curvature angle improves heat release rates, which ultimately results in a higher solidification rate throughout the system. The results suggest that augmenting the curvature of arc-shaped fins from 60° to 120° and 180° will bring solidifying time savings of about 10.3% and 22.1%, respectively, while also improving the heat recovery rates by about 12.9% and 32.0%.
- (2) Increasing the spacing of the fin base from 5 to 10 or 15 mm will result in solidifying time savings of 9.1% and 14.5% while increasing the heat recovery rates by about 13.7% and 20.9%, respectively. The data for augmenting the joining angle between the upper arc-shaped fins from 0° to 30° or 60° return a reduction in solidifying time of about 15.4% and 25.9%, respectively. This alteration stimulates faster heat recovery rates of roughly 18.6% to 34.7%, respectively.
- (3) Augmenting the angle between the bottom fin segments results in a negative flow-assisting environment for arc-shaped fin arrays, thereby rendering them less beneficial for intensifying the heat removal rates through natural convection. The data for reducing the joining angle between the bottom arc-shaped fins from 120° to 60° or 30° indicates a reduction in solidifying time of approximately 31.3% and 29.2%, respectively. This alteration would also result in an increase in heat recovery rates of roughly 44.1% and 40.1%, respectively. Therefore, choosing a suitable joining angle between the top and bottom fins can significantly improve the solidification behavior of PCMs and can enhance their heat recovery rates.
- (4) Selecting an optimized array of arc-shaped fins can achieve significant improvements compared to + - shaped fins, which are commonly used in thermal energy storage applications. Under the condition that a constant volume is maintained for the fins in both cases, the case of arc-shaped fins reveals potential to reduce the solidifying time by 65.1% and increase the heat storage rate by 190.5%, while + - shaped fins can only achieve 34.4% and 51.8% improvements, respectively. This superior performance of arc-shaped fins can be attributed to their flow-enhancing structure, which significantly improves the role of convection in expediting the heat removal process.

These findings indicate that arc-shaped fins are a promising design for enhancing the discharge performance of PCM-based energy storage systems.

## Acknowledgment

The corresponding author (AK) would like to acknowledge the funding by the UK Engineering and Physical Sciences Research Council (EPSRC – Reference: EP/X525753/1) under the Impact Acceleration Account provided to the University of Manchester, which has supported the underpinning research in this collaborative study with direct input from the industrial partners involved in the above project.

## Disclosure statement

No potential conflict of interest was reported by the author(s).

## References

- Abdulateef, A. M., Abdulateef, J., Mat, S., Sopian, K., Elhub, B., & Mussa, M. A. (2018). Experimental and numerical study of solidifying phase-change material in a triplex-tube heat exchanger with longitudinal/triangular fins. *International Communications in Heat and Mass Transfer*, 90, 73–84. <https://doi.org/10.1016/j.icheatmasstransfer.2017.10.003>
- Agyenim, F., Eames, P., & Smyth, M. (2009). A comparison of heat transfer enhancement in a medium temperature thermal energy storage heat exchanger using fins. *Solar Energy*, 83(9), 1509–1520. <https://doi.org/10.1016/j.solener.2009.04.007>
- Al-Abidi, A. A., Mat, S., Sopian, K., Sulaiman, M. Y., & Mohammad, A. T. (2014). Experimental study of melting and solidification of PCM in a triplex tube heat exchanger with fins. *Energy and Buildings*, 68, 33–41. <https://www.sciencedirect.com/science/article/pii/S0378778813005707>
- Amano, R., & Sundén, B. (2011). *Computational fluid dynamics and heat transfer: Emerging topics* (Vol. 23). WIT Press.
- Ao, C., Yan, S., Zhao, X., Zhang, N., & Wu, Y. (2023). Design optimization of a novel annular fin on a latent heat storage device for building heating. *Journal of Energy Storage*, 64, 107124. <https://www.sciencedirect.com/science/article/pii/S2352152X23005212>
- Bahlekeh, A., Mohammed, H. I., Al-Azzawi, W. K., Dulaimi, A., Majdi, H. S., Talebizadehsardari, P., & Mahdi, J. M. (2022). CFD analysis on optimizing the annular fin parameters toward an improved storage response in a triple-tube containment system. *Energy Science & Engineering*, n/a(n/a), <https://onlinelibrary.wiley.com/doi/abs/10.1002/ese3.1310>
- Bo, L., Mahdi, J. M., Rahbari, A., Majdi, H. S., Xin, Y., Yäici, W., & Talebizadehsardari, P. (2022). Twisted-fin parametric study to enhance the solidification performance of phase-change material in a shell-and-tube latent heat thermal energy storage system. *Journal of Computational Design and Engineering*, 2297. <https://doi.org/10.1093/jcde/qwac107>
- Brent, A., Voller, V., & Reid, K. (1988). Enthalpy-porosity technique for modeling convection-diffusion phase change: Application to the melting of a pure metal. *Numerical Heat Transfer, Part A Applications*, 13(3), 297–318.
- Cabeza, L. F. (2021). *Advances in thermal energy storage systems: Methods and applications*. Elsevier.

- Darbari, B., Rashidi, S., & Keshmiri, A. (2020). Nanofluid heat transfer and entropy generation inside a triangular duct equipped with delta winglet vortex generators. *Journal of Thermal Analysis and Calorimetry*, 140(3), 1045–1055. <https://doi.org/10.1007/s10973-019-08382-7>
- Darzi, A. A., Jourabian, M., & Farhadi, M. (2016). Melting and solidification of PCM enhanced by radial conductive fins and nanoparticles in cylindrical annulus. *Energy Conversion and Management*, 118, 253–263. <https://www.sciencedirect.com/science/article/pii/S019689041630259X>
- Du, Z., Liu, G., Huang, X., Xiao, T., Yang, X., & He, Y.-L. (2023). Numerical studies on a fin-foam composite structure towards improving melting phase change. *International Journal of Heat and Mass Transfer*, 208, 124076. <https://www.sciencedirect.com/science/article/pii/S0017931023002296>
- Ghalambaz, M., Groşan, T., & Pop, I. (2019). Mixed convection boundary layer flow and heat transfer over a vertical plate embedded in a porous medium filled with a suspension of nano-encapsulated phase change materials. *Journal of Molecular Liquids*, 293, 111432. <https://doi.org/10.1016/j.molliq.2019.111432>
- GmbH. Product information, data sheet of RT35 by Rubitherm GmbH.
- Gong, D., Wei, C., Xie, D., & Tang, Y. (2022). Ultrasmall antimony nanodots embedded in carbon nanowires with three-dimensional porous structure for high-performance potassium dual-ion batteries. *Chemical Engineering Journal*, 431, 133444. <https://doi.org/10.1016/j.cej.2021.133444>
- Hassan, A. K., Abdulateef, J., Mahdi, M. S., & Hasan, A. F. (2020). Experimental evaluation of thermal performance of two different finned latent heat storage systems. *Case Studies in Thermal Engineering*, 21, 100675. <https://doi.org/10.1016/j.csite.2020.100675>
- Hosseini, M., Ranjbar, A., Rahimi, M., & Bahrampoury, R. (2015). Experimental and numerical evaluation of longitudinally finned latent heat thermal storage systems. *Energy and Buildings*, 99, 263–272. <https://doi.org/10.1016/j.enbuild.2015.04.045>
- Hosseinzadeh, K., Montazer, E., Shafii, M. B., & Ganji, A. (2021). Solidification enhancement in triplex thermal energy storage system via triplets fins configuration and hybrid nanoparticles. *Journal of Energy Storage*, 34, 102177. <https://doi.org/10.1016/j.est.2020.102177>
- Huang, G., Curt, S. R., Wang, K., & Markides, C. N. (2020). Challenges and opportunities for nanomaterials in spectral splitting for high-performance hybrid solar photovoltaic-thermal applications: A review. *Nano Materials Science*, 2(3), 183–203. <https://www.sciencedirect.com/science/article/pii/S2589965120300106>
- IEA. (2023). *CO2 Emissions in 2022*, <https://www.iea.org/reports/co2-emissions-in-2022>
- IRENA. (2020a). *Global renewables outlook: Energy Transformation 2050*. ISBN 978-92-9260-238-3.
- IRENA. (2020b). *Innovation outlook: Thermal energy storage, international renewable energy agency, Abu Dhabi*.
- Karar, O., Emami, S., Marappa Gounder, R., Myo Thant, M. M., Mukhtar, H., Sharifpur, M., & Sadeghzadeh, M. (2021). Experimental and numerical investigation on convective heat transfer in actively heated bundle-pipe. *Engineering Applications of Computational Fluid Mechanics*, 15(1), 848–864. <https://doi.org/10.1080/19942060.2021.1920466>
- Keshmiri, A., Uribe, J., & Shokri, N. (2015). Benchmarking of three different CFD codes in simulating natural, forced, and mixed convection flows. *Numerical Heat Transfer, Part A: Applications*, 67(12), 1324–1351. <https://doi.org/10.1080/10407782.2014.965115>
- Khedher, N. B., Togun, H., Abed, A. M., Mohammed, H. I., Mahdi, J. M., Ibrahim, R. K., ... Keshmiri, A. (2023). Comprehensive analysis of melting enhancement by circular Y-shaped fins in a vertical shell-and-tube heat storage system. *Engineering Applications of Computational Fluid Mechanics*, 17(1), 2227682. <https://doi.org/10.1080/19942060.2023.2227682>
- Khosravi, K., Eisapour, A. H., Rahbari, A., Mahdi, J. M., Talebizadehsardari, P., & Keshmiri, A. (2023). Photovoltaic-thermal system combined with wavy tubes, twisted tape inserts and a novel coolant fluid: Energy and exergy analysis. *Engineering Applications of Computational Fluid Mechanics*, 17(1), 2208196. <https://doi.org/10.1080/19942060.2023.2208196>
- Lane, G. A. (1983). *Solar heat storage: latent heat materials* (Vol. 1).
- Li, F., Huang, X., Li, Y., Lu, L., Meng, X., Yang, X., & Sundén, B. (2023). Application and analysis of flip mechanism in the melting process of a triplex-tube latent heat energy storage unit. *Energy Reports*, 9, 3989–4004. <https://www.sciencedirect.com/science/article/pii/S235248472300269X>
- Lu, B., Meng, X., Zhu, M., & Suzuki, R. O. (2018). Thermoelectric system absorbing waste heat from a steel ladle. *Journal of Electronic Materials*, 47(6), 3238–3247. <https://doi.org/10.1007/s11664-018-6073-4>
- Mahdi, J. M., Lohrasbi, S., Ganji, D. D., & Nsofor, E. C. (2018). Accelerated melting of PCM in energy storage systems via novel configuration of fins in the triplex-tube heat exchanger. *International Journal of Heat and Mass Transfer*, 124, 663–676. <https://www.sciencedirect.com/science/article/pii/S0017931017333355>
- Mahdi, J. M., Lohrasbi, S., Ganji, D. D., & Nsofor, E. C. (2019). Simultaneous energy storage and recovery in the triplex-tube heat exchanger with PCM, copper fins and Al<sub>2</sub>O<sub>3</sub> nanoparticles. *Energy Conversion and Management*, 180, 949–961. <http://www.sciencedirect.com/science/article/pii/S0196890418312895>
- Mahdi, J. M., & Nsofor, E. C. (2018). Solidification enhancement of PCM in a triplex-tube thermal energy storage system with nanoparticles and fins. *Applied Energy*, 211, 975–986. <http://www.sciencedirect.com/science/article/pii/S0306261917316811>
- Mashayekhi, R., Arasteh, H., Toghraie, D., Motaharpour, S. H., Keshmiri, A., & Afrand, M. (2020). Heat transfer enhancement of Water-Al<sub>2</sub>O<sub>3</sub> nanofluid in an oval channel equipped with two rows of twisted conical strip inserts in various directions: A two-phase approach. *Computers & Mathematics with Applications*, 79(8), 2203–2215. <https://doi.org/10.1016/j.camwa.2019.10.024>
- Mashayekhi, R., Eisapour, A. H., Eisapour, M., Talebizadehsardari, P., & Rahbari, A. (2022). Hydrothermal performance of twisted elliptical tube equipped with twisted tape insert. *International Journal of Thermal Sciences*, 172, 107233. <https://doi.org/10.1016/j.ijthermalsci.2021.107233>
- Menni, Y., Ameer, H., Sharifpur, M., & Ahmadi, M. H. (2021). Effects of in-line deflectors on the overall performance of a channel heat exchanger. *Engineering Applications of*



- Computational Fluid Mechanics*, 15(1), 512–529. <https://doi.org/10.1080/19942060.2021.1893820>.
- Mozafari, M., Hooman, K., Lee, A., & Cheng, S. (2022). Numerical study of a dual-PCM thermal energy storage unit with an optimized low-volume fin structure. *Applied Thermal Engineering*, 215, 119026. <https://www.sciencedirect.com/science/article/pii/S1359431122009607>
- Mozafari, M., Lee, A., & Cheng, S. (2022). A novel dual-PCM configuration to improve simultaneous energy storage and recovery in triplex-tube heat exchanger. *International Journal of Heat and Mass Transfer*, 186, 122420. <https://www.sciencedirect.com/science/article/pii/S0017931021015180>
- Nie, C., Deng, S., & Liu, J. (2020). Effects of fins arrangement and parameters on the consecutive melting and solidification of PCM in a latent heat storage unit. *Journal of Energy Storage*, 29, 101319. <http://www.sciencedirect.com/science/article/pii/S2352152X19313726>
- Peng, H., Yan, W., Wang, Y., & Feng, S. (2022). Discharging process and thermal evaluation in the thermal energy storage system with fractal tree-like fins. *International Journal of Heat and Mass Transfer*, 183, 122073. <https://doi.org/10.1016/j.jheatmasstransfer.2021.122073>
- Rajabifar, B., Seyf, H. R., Zhang, Y., & Khanna, S. K. (2016). Flow and heat transfer in micro Pin Fin heat sinks With nano-encapsulated phase change materials. *Journal of Heat Transfer*, 138(6), 062401. <https://doi.org/10.1115/1.4032834>
- Rashid, F. L., Rahbari, A., Ibrahim, R. K., Talebizadehsardari, P., Basem, A., Kaoood, A., ... Al-Obaidi, M. A. (2023). Review of solidification and melting performance of phase change materials in the presence of magnetic field, rotation, tilt angle, and vibration. *Journal of Energy Storage*, 67, 107501. <https://www.sciencedirect.com/science/article/pii/S2352152X23008988>
- Rathod, M. K., & Banerjee, J. (2015). Thermal performance enhancement of shell and tube latent heat storage unit using longitudinal fins. *Applied Thermal Engineering*, 75, 1084–1092. <https://doi.org/10.1016/j.applthermaleng.2014.10.074>
- Sciakovelli, A., Gagliardi, F., & Verda, V. (2015). Maximization of performance of a PCM latent heat storage system with innovative fins. *Applied Energy*, 137, 707–715. <https://doi.org/10.1016/j.apenergy.2014.07.015>
- Shamsabadi, H., Rashidi, S., Esfahani, J. A., & Keshmiri, A. (2020). Condensation in the presence of non-condensable gases in a convergent 3D channel. *International Journal of Heat and Mass Transfer*, 152, 119511. <https://doi.org/10.1016/j.jheatmasstransfer.2020.119511>
- Song, S., Chong, D., Zhao, Q., Chen, W., & Yan, J. (2023). Numerical investigation of the condensation oscillation mechanism of submerged steam jet with high mass flux. *Chemical Engineering Science*, 270, 118516. <https://doi.org/10.1016/j.ces.2023.118516>
- Tang, S.-Z., Tian, H.-Q., Zhou, J.-J., & Li, H. (2021). Evaluation and optimization of melting performance in a horizontal thermal energy storage unit with non-uniform fins. *Journal of Energy Storage*, 33, 102124. <https://www.sciencedirect.com/science/article/pii/S2352152X20319526>
- Tao, Y. B., Liu, Y. K., & He, Y.-L. (2017). Effects of PCM arrangement and natural convection on charging and discharging performance of shell-and-tube LHS unit. *International Journal of Heat and Mass Transfer*, 115(Part B), 99–107. <http://www.sciencedirect.com/science/article/pii/S0017931017313613>
- Wang, G.-G., Gao, D., & Pedrycz, W. (2022). Solving multi-objective fuzzy job-shop scheduling problem by a hybrid adaptive differential evolution algorithm. *IEEE Transactions on Industrial Informatics*, 18(12), 8519–8528.
- Wang, H., Fu, F., Huang, M., Feng, Y., Han, D., Xi, Y., ... Niu, L. (2023). Lignin-based materials for electrochemical energy storage devices. *Nano Materials Science*, 5(2), 141–160. <https://www.sciencedirect.com/science/article/pii/S2589965122000022>
- Wang, L., Lei, Y., Du, B., Li, Y., & Sun, J. (2023). Performance enhancement of a horizontal latent thermal energy storage unit with elliptical fins. *Applied Thermal Engineering*, 225, 120191. <https://www.sciencedirect.com/science/article/pii/S135943112300220X>
- Wang, M., Jiang, C., Zhang, S., Song, X., Tang, Y., & Cheng, H.-M. (2018). Reversible calcium alloying enables a practical room-temperature rechargeable calcium-ion battery with a high discharge voltage. *Nature Chemistry*, 10(6), 667–672. <https://doi.org/10.1038/s41557-018-0045-4>
- Wen, Q., He, X., Lu, Z., Streiter, R., & Otto, T. (2021). A comprehensive review of miniaturized wind energy harvesters. *Nano Materials Science*, 3(2), 170–185. <https://www.sciencedirect.com/science/article/pii/S2589965121000180>
- Wu, X., Li, C., Zhou, Z., Nie, X., Chen, Y., Zhang, Y., ... Said, Z. (2021). Circulating purification of cutting fluid: An overview. *The International Journal of Advanced Manufacturing Technology*, 117(9), 2565–2600. <https://doi.org/10.1007/s00170-021-07854-1>
- Wu, Y., Li, D., Jiang, W., Zhu, S., Zhao, X., Arıcı, M., & Tunçbilek, E. (2022). Energy storage and exergy efficiency analysis of a shell and tube latent thermal energy storage unit with non-uniform length and distributed fins. *Sustainable Energy Technologies and Assessments*, 53, 102362. <https://www.sciencedirect.com/science/article/pii/S2213138822004143>
- Wu, Y., Zhao, Y., Han, X., Jiang, G., Shi, J., Liu, P., ... Jin, Z. (2021). Ultra-fast growth of cuprate superconducting films: Dual-phase liquid assisted epitaxy and strong flux pinning. *Materials Today Physics*, 18, 100400. <https://doi.org/10.1016/j.mtphys.2021.100400>
- Xu, Y., Chen, X., Zhang, H., Yang, F., Tong, L., Yang, Y., ... Liu, Z. (2022). Online identification of battery model parameters and joint state of charge and state of health estimation using dual particle filter algorithms. *International Journal of Energy Research*, 46(14), 19615–19652.
- Yang, X., Lu, Z., Bai, Q., Zhang, Q., Jin, L., & Yan, J. (2017). Thermal performance of a shell-and-tube latent heat thermal energy storage unit: Role of annular fins. *Applied Energy*, 202, 558–570. <https://doi.org/10.1016/j.apenergy.2017.05.007>
- Zandie, M., Moghaddas, A., Kazemi, A., Ahmadi, M., Feshkache, H. N., Ahmadi, M. H., & Sharifpur, M. (2022). The impact of employing a magnetic field as well as Fe<sub>3</sub>O<sub>4</sub> nanoparticles on the performance of phase change materials. *Engineering Applications of Computational Fluid Mechanics*, 16(1), 196–214. <https://doi.org/10.1080/19942060.2021.2006092>
- Zhang, J., Cao, Z., Huang, S., Huang, X., Han, Y., Wen, C., ... Yang, Y. (2023). Solidification performance improvement of phase change materials for latent heat thermal energy storage using novel branch-structured fins and



- nanoparticles. *Applied Energy*, 342, 121158. <https://www.sciencedirect.com/science/article/pii/S0306261923005226>
- Zhang, S., Mancin, S., & Pu, L. (2023). A review and prospective of fin design to improve heat transfer performance of latent thermal energy storage. *Journal of Energy Storage*, 62, 106825. <https://www.sciencedirect.com/science/article/pii/S2352152X23002220>
- Zhao, Y., Zhang, B., Hou, H., Chen, W., & Wang, M. (2019). Phase-field simulation for the evolution of solid/liquid interface front in directional solidification process. *Journal of Materials Science & Technology*, 35(6), 1044–1052. <https://doi.org/10.1016/j.jmst.2018.12.009>